Contract NAS9-16985

NEAR FIELD TO FAR FIELD TRANSFORMATIONS AND MULTIPLE BEAM FORMING AND STEERING

FINAL REPORT

Prepared For:

National Aeronautics and Space Administration
Lyndon B. Johnson Space Center

November 19, 1984

Prepared by:

Novar Electronics Corporation
24 Brown Street
Barberton, Ohio 44203

NOVAR®

Contract NAS9-16985

NEAR FIELD TO FAR FIELD TRANSFORMATIONS AND MULTIPLE BEAM FORMING AND STEERING

FINAL REPORT

Prepared For:

National Aeronautics and Space Administration
Lyndon B. Johnson Space Center

November 19, 1984

Prepared by:

Novar Electronics Corporation
24 Brown Street
Barberton, Ohio 44203

TABLE OF CONTENTS

SECTION I

NEAR FIELD TO FAR FIELD TRANSFORMATIONS

1.0 Introduction

1.1 Background

Near field measurements to determine far field patterns of antennas are felt to be an effective alternative to far field range measurements.[1,2,3]

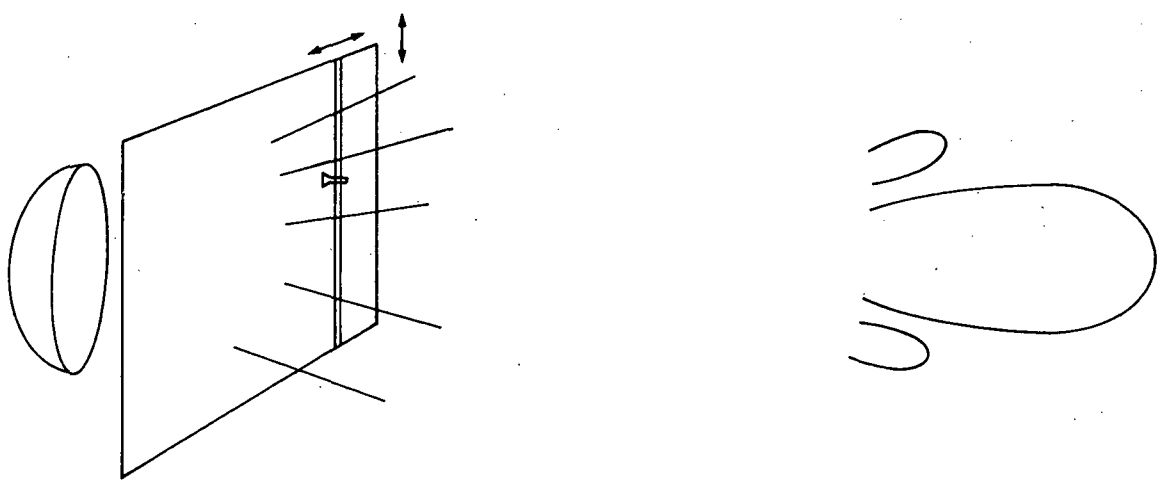

FIGURE 1

FAR FIELD ANTENNA PATTERNS FROM

NEAR FIELD MEASUREMENTS

This is especially true for microwave antennas and most especially for phased array antennas. Near field measurements allow measurements to be made indoors. An indoor range provides the all-weather capability to enable tests to be performed in a controlled environment. In addition, large-antenna logistics and mounting problems are simplified by near field measurement systems. These systems are felt to be time and cost effective, with accuracy comparable to that of far field ranges. The requirements for a more complicated and expensive measurement system with more expensive probe calibration are not felt by proponents to be serious disadvantages.

1.2 Project Objectives

As a part of this contract, the feasibility of acoustic verification of microwave near field to far field transformation algorithms using the Phased Array Sonic Simulation System was studied. Existing electromagnetic near field measurement techniques and transformation algorithms (equations) were investigated.[1,2,3,4] It was analytically determined that acoustic verification is valid. ~~We would like to explicitly point out that although far field patterns from near field patterns for acoustic arrays are valid[6,7] (and in fact may have been the earliest use of near field to far field transformations), what we are talking about here is~~ acoustic simulation of electromagnetic

near field to far field transformations. One merely needs to separately simulate acoustically the transmission of the two orthogonal polarization components of the EM wave and then superimpose the results to get the analytical description of the total field.

The acoustic simulation of electromagnetic near field to far field transformation is verified for the "modal expansion" method.[1,4,9] In the modal expansion method, data from antenna near field measurements are converted to a summation or spectrum of modes corresponding to wave numbers in the measurement coordinate system.[1] With a rectangular coordinate system, the field at all points in front of a plane aperture of any aperture distribution may be regarded as arising from an aggregate of plane waves traveling in various directions. The amplitude and phase of the waves as a function of their direction of travel constitutes an angular spectrum.[5] Another way of looking at the same thing, and this is the philosopical approach taken in the verification method used in this report, is that all the far field pattern information is contained in the near field and thus is contained in measurements made in the near field. Fourier transformation of those measurements preserves the far field information is a spectral form that is then readily extractable.

NEAR FIELDS
FAR FIELDS
ANTENNA RADIATION PATTERNS
ELECTROMAGNETIC MEASUREMENTS
ACOUSTIC SIMULATION

FAST FOURIER TRANSFORMATION
ELECTROMAGNETIC WAVE TRANSMISSION
WAVE EQUATION
PLANE WAVES
MULTIBEAM ANTENNAS

MICROWAVE ANTENNAS
PHASED ARRAYS
ALGORITHMS
ACOUSTIC MEASUREMENTS

1.3 Near Field/Far Field Definitions

Before presenting the details of the mathematical verification, it is important to define what we mean by near field and far field. It is commonly accepted[8] that the far field is that region which is at a distance from the antenna greater than

$$\frac{2D^2}{\lambda} \tag{1}$$

where D is the largest dimension of the antenna and λ is the wavelength. The near field is the near radiating field and is the region between the far field and the near reactive field. The near field is considered by many to begin at a distance from the antenna greater than

$$\lambda/2\pi.$$

However[10] this defines the point where the reactive near field equals the radiating near field for a small dipole. Suffice to say that for most antennas, that point is usually less than a few wavelengths from the antenna. Thus near field measurements are usually made within a few wavelengths from the antenna. Strictly speaking, there is nothing in the verfication proof to be developed below that restricts the measurement plane to <u>any</u> region or distance.

2.0 Near Field to Far Field Transformation - Mathematical Verification

2.1 Wave Equation Basis

Consider the well known wave equation governing electromagnetic radiation in a source-free region and given in terms of the time-varying electric field vector, $\underline{E}$:

$$\nabla^2 \underline{E} = \mu\varepsilon \frac{\partial^2}{\partial t^2} \underline{E}, \qquad (2)$$

where ∇^2 is the Laplacian operator. For a monochromatic (ie., single frequency) field,

$$\underline{E} = \text{Real } \{\hat{\underline{E}} e^{j\omega t}\} \qquad (3)$$

where the "hat" denotes the phasor. Let the coordinate systems of interest be defined by Figure 2. Substitution

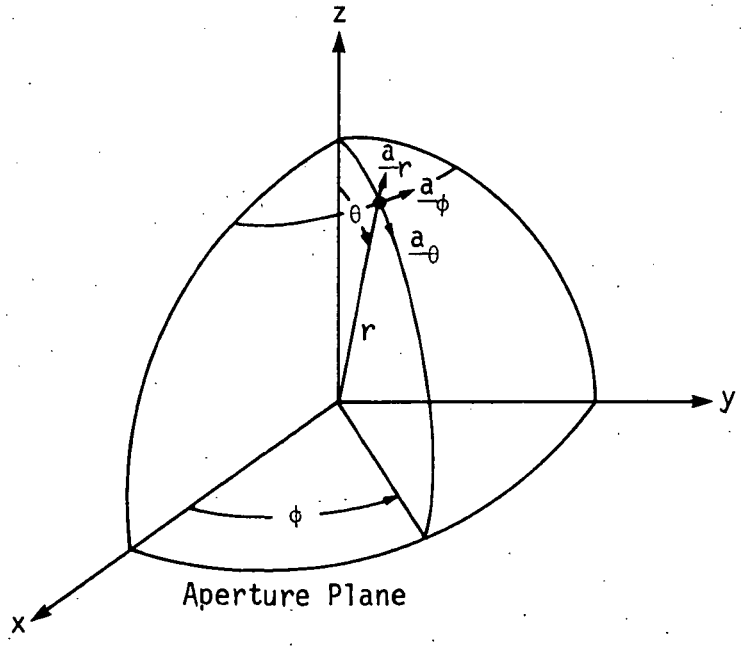

FIGURE 2

COORDINATES DIAGRAM

of (3) into (2) then yields

$$\nabla^2 \underline{E} = -\mu\varepsilon\omega^2 \hat{\underline{E}}. \tag{4}$$

Let us express $\hat{\underline{E}}$ and ∇^2 in rectangular coordinates:

$$\hat{\underline{E}} = \hat{\underline{E}}\ (x,y,z)$$

$$\nabla^2 = \frac{\partial^2}{\partial x^2} + \frac{\partial^2}{\partial y^2} + \frac{\partial^2}{\partial z^2}\ .$$

The propagation velocity, c, is given by

$$c = \frac{1}{\sqrt{\mu\varepsilon}}\ .$$

Since

$$c = f\lambda,$$

where f is the frequency, the wave equation as described by (4) can be rewritten as

$$\nabla^2 \hat{\underline{E}} = -k^2 \hat{\underline{E}} \tag{5}$$

where k is the propagation constant (wave number) expressed by:

$$k = 2\pi/\lambda.$$

Let us now take a two-dimensional Fourier transform with respect to the x and y dimensions of the wave equation. Taking such a Fourier transform of both sides of (5) yields

$$\int_{-\infty}^{\infty}\{\int_{-\infty}^{\infty}[\nabla^2\hat{\underline{E}}(x,y,z)]e^{-jk_x x}dx\}e^{-jk_y y}dy$$

$$= \int_{-\infty}^{\infty}\{\int_{-\infty}^{\infty}[-k^2\hat{\underline{E}}(x,y,z)]e^{-jk_x x}dx\}e^{-jk_y y}dy \qquad (6)$$

where k_x and k_y can be thought of as spatial frequencies. Using the rectangular coordinates' expression for the Laplacian operator, ∇^2, (6) becomes

$$\int_{-\infty}^{\infty}\{\int_{-\infty}^{\infty}[\frac{\partial^2}{\partial x^2}\hat{\underline{E}}(x,y,z)]e^{-jk_x x}dx\}e^{-jk_y y}dy$$

$$+ \int_{-\infty}^{\infty}\{\int_{-\infty}^{\infty}[\frac{\partial^2}{\partial y^2}\hat{\underline{E}}(x,y,z)]e^{-jk_y y}dy\}e^{-jk_x x}dx$$

$$+ \int_{-\infty}^{\infty}\int_{-\infty}^{\infty}[\frac{\partial^2}{\partial z^2}\hat{\underline{E}}(x,y,z)]e^{-j(k_x x + k_y y)}dxdy$$

$$= -k^2\int_{-\infty}^{\infty}\int_{-\infty}^{\infty}\hat{\underline{E}}(x,y,z)e^{-j(k_x x + k_y y)}dxdy. \qquad (7)$$

Let the double-integral term on the right side of the equal sign in (7) be defined as the phasor/vector field, $\hat{\underline{B}}$:

$$\hat{\underline{B}}(k_x,k_y,z) \triangleq \int_{-\infty}^{\infty}\int_{-\infty}^{\infty}\hat{\underline{E}}(x,y,z)e^{-j(k_x x + k_y y)}dxdy. \qquad (8)$$

Note therefore that the third term to the left of the equal sign in (7) then becomes described by (9):

$$\int_{-\infty}^{\infty}\int_{-\infty}^{\infty}\left[\frac{\partial^2}{\partial z^2}\,\hat{\underline{E}}(x,y,z)\right]e^{-j(k_x x + k_y y)}\,dxdy$$

$$= \frac{\partial^2}{\partial z^2}\int_{-\infty}^{\infty}\int_{-\infty}^{\infty}\hat{\underline{E}}(x,y,z)e^{-j(k_x x + k_y y)}\,dxdy$$

$$= \frac{\partial^2}{\partial z^2}\,\hat{\underline{B}}(k_x,k_y,z). \qquad (9)$$

Before examining the first and second terms to the left of the equal sign in (7), let us look at the Fourier transform of differentials. If the Fourier transform of a function, f(t), is given by

$$\mathcal{F}\{f(t)\} = \int_{-\infty}^{\infty} f(t)e^{-j\omega t}dt = F(j\omega), \qquad (10)$$

then f(t) is given by the inverse Fourier transform

$$f(t) = \mathcal{F}^{-1}\{F(j\omega)\} = \frac{1}{2\pi}\int_{-\infty}^{\infty} F(j\omega)e^{j\omega t}d\omega. \qquad (11)$$

Therefore $\mathcal{F}\{\frac{d^n}{dt^n}\,f(t)\}$ is obtained as a direct consequence of taking the n'th derivative of f(t) with respect to t in (11) followed by application of the rule given by (10):

$$\mathcal{F}\{\frac{d^n}{dt^n}\,f(t)\} = (j\omega)^n F(j\omega) = (j\omega)^n \mathcal{F}\{f(t)\}.$$

Thus in the first term of (7) we get

$$\int_{-\infty}^{\infty}\int_{-\infty}^{\infty}\left[\frac{\partial^2}{\partial x^2}\,\hat{\underline{E}}(x,y,z)\right]e^{-jk_x x}\,dx$$

$$= (jk_x)^2\int_{-\infty}^{\infty}\hat{\underline{E}}\,(x,y,z)e^{-jk_x x}\,dx.$$

After taking the Fourier transform with respect to y of this result and using (8), the first term of (7) becomes

$$\int_{-\infty}^{\infty}\{\int_{-\infty}^{\infty}[\frac{\partial^2}{\partial x^2}\hat{\underline{E}}(x,y,z)]e^{-jk_x x}dx\}e^{-jk_y y}dy$$

$$= (jk_x)^2\int_{-\infty}^{\infty}\int_{-\infty}^{\infty}\hat{\underline{E}}(x,y,z)e^{-j(k_x x + k_y y)}dxdy$$

$$= -k_x{}^2\hat{\underline{B}}(k_x,k_y,z). \qquad (12)$$

In a like manner, for the second term in (7), we have:

$$\int_{-\infty}^{\infty}\{\int_{-\infty}^{\infty}[\frac{\partial^2}{\partial y^2}\hat{\underline{E}}(x,y,z)]e^{-jk_y y}dy\}e^{-jk_x x}dx$$

$$= -k_y{}^2\hat{\underline{B}}(k_x,k_y,z). \qquad (13)$$

Substituting the results given by (9), (12), and (13) into (7) gives us the Fourier transformed wave equation in terms of $\hat{\underline{B}}(k_x,k_y,z)$:

$$-k_x{}^2\hat{\underline{B}} - k_y{}^2\hat{\underline{B}} + \frac{\partial^2}{\partial z^2}\hat{\underline{B}} = -k^2\hat{\underline{B}}. \qquad (14)$$

Rearranging terms gives:

$$\frac{\partial^2}{\partial z^2}\hat{\underline{B}}(k_x,k_y,z) = -k_z{}^2\hat{\underline{B}}(k_x,k_y,z) \qquad (15)$$

where

$$k_z^2 \triangleq k^2 - k_z^2 - k_y^2. \tag{16}$$

Equation (15) has a solution given by

$$\hat{\underline{B}}\,(k_x,k_y,z) = \hat{\underline{A}}\,(k_x,k_y)e^{jk_z z}. \tag{17}$$

(Proof is by substitution, which can almost be seen by inspection.) (Note that:

$$\hat{\underline{A}}\,(k_x,k_y) = \hat{\underline{B}}\,(k_x,k_y,\,0).)$$

Since $\hat{\underline{B}}\,(k_x,k_y,z)$ as given by (8) is seen to be a two-dimensional Fourier transform of $\hat{\underline{E}}$ with respect to x and y, then the uniqueness property of Fourier transform pairs means that $\hat{\underline{E}}(x,y,z)$ is given by the inverse Fourier transform:

$$\hat{\underline{E}}(x,y,z) = \left(\frac{1}{2\pi}\right)^2 \int_{-\infty}^{\infty}\int_{-\infty}^{\infty} \hat{\underline{B}}\,(k_x,k_y,z)e^{j(k_x x + k_y y)}\,dk_x dk_y. \tag{18}$$

Using the wave equation solution given in terms of $\hat{\underline{B}}$ expressed by (17), (18) becomes:

$$\hat{\underline{E}}(x,y,z) = \frac{1}{4\pi^2}\int_{-\infty}^{\infty}\int_{-\infty}^{\infty}\left[\hat{\underline{A}}(k_x,k_y)e^{jk_z z}\right]e^{j(k_x x + k_y y)}\,dk_x dk_y. \tag{19a}$$

The result given by (19a) can be expressed in compact vector notation as:

$$\hat{\underline{E}}(\underline{r}) = \frac{1}{4\pi^2}\int_{-\infty}^{\infty}\int_{-\infty}^{\infty} \hat{\underline{A}}\,(k_x,k_y)e^{j\underline{k}\,\cdot\,\underline{r}}\,dk_x dk_y \tag{19b}$$

where $\underline{k} = k_x\underline{a}_x + k_y\underline{a}_y + k_z\underline{a}_z$,

$$\underline{r} = x\underline{a}_x + y\underline{a}_y + z\underline{a}_z,$$

and $\underline{a}_x$, $\underline{a}_y$, $\underline{a}_z$ are unit direction vectors.

2.2 Physical Concepts/Terminology

Let us now look at the physical significance of the terms in the expression for the electric field given by (19b):

- $\hat{\underline{E}}(r)$ is the electric field, expressed as a vector intensity, defined by $\underline{r}$, the magnitude and direction of that point from origin of the coordinate system.
- $\hat{\underline{A}}(k_x,k_y)e^{j\underline{k}\cdot\underline{r}}$ is an expression for a plane wave.
- $\hat{\underline{A}}(k_x,k_y)$ is a plane wave spectrum. This arises from the fact that the form of (17b) shows that $\hat{\underline{E}}$ is the inverse Fourier transform of $\hat{\underline{A}}$. Therefore $\hat{\underline{A}}$ is the Fourier transform (and therefore the spectrum) of $\hat{\underline{E}}$:

$$\hat{\underline{A}}(k_x,k_y) = \int_{-\infty}^{\infty}\int_{-\infty}^{\infty} \hat{\underline{E}}(x,y,z)e^{-j\underline{k}\cdot\underline{r}}\,dxdy.$$

- $\int_{-\infty}^{\infty}\int_{-\infty}^{\infty}\underline{A}(k_x,k_y)e^{j\underline{k}\cdot\underline{r}}\,dk_x dk_y$ is a superposition (sum) of plane waves of every "mode" k_x, k_y.

The field $\hat{\underline{E}}(\underline{r})$ is therefore expressed as a "modal expansion" (a "plane wave expansion") by (19b.) This equation shows

that the field may be regarded as being made up of a superposition of plane waves.

2.3 Propagating/Evanescent Plane Waves

From (19a) and (19b) we use the relationship

$$\underline{A}(k_x.k_y)e^{j\underline{k}\cdot\underline{r}} = [\underline{A}(k_x,k_y)e^{j(k_x x + k_y y)}]e^{jk_z z}.$$

We see that the exponential term in z can be expressed as

$$e^{jk_z z} = e^{-\gamma z}$$

where γ is the propagation constant and where from (16) we have

$$k_z = \sqrt{k^2 - k_x^2 - k_y^2}. \qquad (20)$$

In general, γ is composed of real and imaginary parts, the attenuation and phase constants, respectively:

$$-jk_z = \gamma = \alpha + j\beta, \qquad (21)$$

where α and β are real numbers. In (16) then, when

$$k_x^2 + k_y^2 > k^2,$$

k_z is imaginary. This means that k_z can be represented as

$$k_z = j\alpha,$$

and therefore

$$e^{jk_z z} = e^{-\alpha z}, \text{ for } k_z \text{ imaginary.}$$

Thus we see that those waves for which k_z is imaginary will "evanesce" (attenuate rapidly to zero in a direction toward the far field). When

$$k_x^2 + k_y^2 < k^2,$$

k_z is real and can be represented (choosing the minus value for the square root radical) as

$$k_z = -\beta.$$

Therefore in this case,

$$e^{jk_z z} = e^{-j\beta z}.$$

The term $e^{-j\beta z}$ is merely a phase term. Thus those waves for which k_z is real will <u>propagate</u> (will exist at infinite values of z, the far field).

Thus from (19b) we see that the electric field is made up of a superposition of propagating and evanescent plane waves.

2.4 Near Field Measurements

In a plane parallel to and located at a distance, z_o, from the aperture plane, the electric field, $\hat{\underline{E}}$ as represented by (19a), is given by

$$\hat{\underline{E}}(x,y,z_o) = \frac{1}{4\pi^2}\int_{-\infty}^{\infty}\int_{-\infty}^{\infty}[\hat{\underline{A}}(k_x,k_y)e^{jk_z z_o}]e^{j(k_x x + k_y y)}\,dk_x dk_y.$$

Therefore the uniqueness of Fourier transform pairs dictates that:

$$\hat{\underline{A}}(k_x,k_y)e^{jk_z z_o} = \int_{-\infty}^{\infty}\int_{-\infty}^{\infty}\hat{\underline{E}}(x,y,z_o)e^{-j(k_x x + k_y y)}\,dxdy. \quad (22)$$

Thus the plane wave spectrum, $\hat{\underline{A}}$, can be calculated (using (22)) from measurements of the electric field, $\hat{\underline{E}}(x,y,z_o)$, made in that plane:

$$\hat{\underline{A}}(k_x,k_y) = e^{-jk_z z_o}\int_{-\infty}^{\infty}\int_{-\infty}^{\infty}\hat{\underline{E}}(x,y,z_o)e^{-j(k_x x + k_y y)}\,dxdy. \quad (23)$$

Equation (23) is valid irrespective of the magnitude of z_o. Thus $\hat{\underline{A}}$ can be determined from measurements made at a distance, z_o, which puts that plane in the near field of the antenna (see Figure 3). Once we have calculated $\hat{\underline{A}}$ from such near

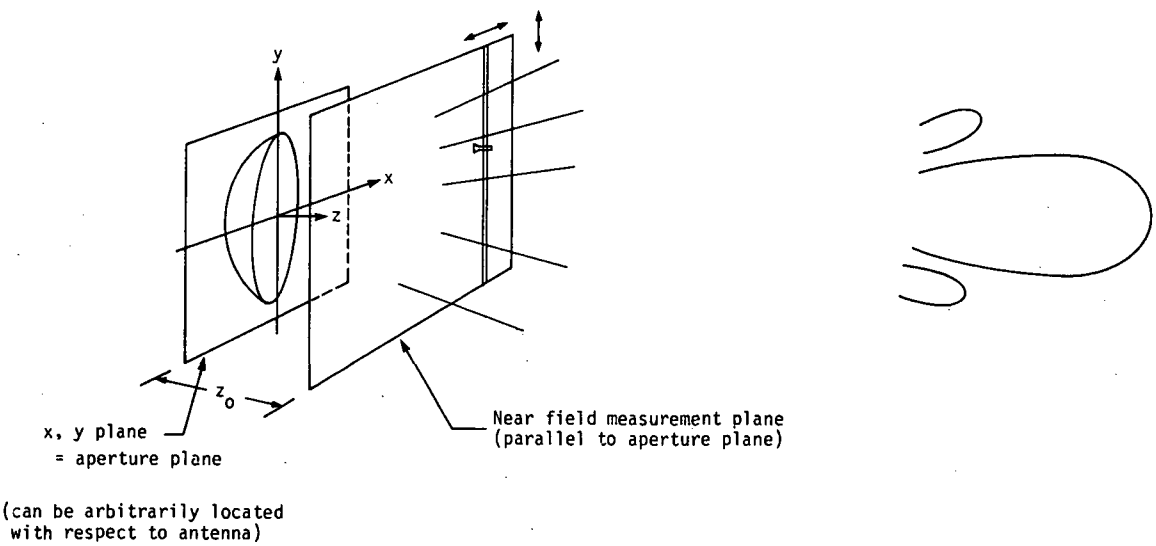

FIGURE 3

ORIENTATION OF MEASUREMENT PLANE

field measurements, we can then determine the electric field, $\hat{\underline{E}}$, for any $\underline{r}(x,y,z)$ in Equation (19b). This is, we can determine $\hat{\underline{E}}$ anywhere by substitution of the result of the calculation of $\hat{\underline{A}}$ from (23) into (19b):

$$\hat{\underline{E}}(x,y,z) = \frac{1}{4\pi^2} \int_{-\infty}^{\infty}\int_{-\infty}^{\infty} \hat{\underline{A}}(k_x,k_y) e^{j\underline{k} \cdot \underline{r}} \, dk_x dk_y. \qquad (19b)$$

"Anywhere", of course, includes the far field which is what we're especially interested in here.

The electric field, $\hat{\underline{E}}(x,y,z)$, in the far field (the "far field" pattern) can be evaluated by evaluating $\hat{\underline{A}}(k_x,k_y)$ in (19b) at particular values of k_x and k_y. The method of "stationary phase"[7] can be used to derive the result. We will use that method below. But first, let us derive some useful relationships.

2.5 Field Relationships

The electric field, $\hat{\underline{E}}$, and its corresponding plane wave spectrum, $\hat{\underline{A}}$, can be expressed vectorially in rectangular coordinates in terms of the unit direction vectors and directional phasor components to have (19b) yield:

$$\hat{\underline{E}}(x,y,z) = \underline{a}_x \hat{E}_x(x,y,z) + \underline{a}_y \hat{E}_y(x,y,z) + \underline{a}_z \hat{E}_z(x,y,z)$$

$$= \frac{1}{4\pi^2} \int_{-\infty}^{\infty}\int_{-\infty}^{\infty} [\underline{a}_x \hat{A}_x(x,y,z) + \underline{a}_y \hat{A}_y(x,y,z)$$

$$+ \underline{a}_z \hat{A}_z(x,y,z)] e^{j\underline{k} \cdot \underline{r}} \, dk_x dk_y.$$

Therefore we have the triad

$$\hat{E}_x(x,y,z) = \frac{1}{4\pi^2}\int_{-\infty}^{\infty}\int_{-\infty}^{\infty}\hat{A}_x(k_x,k_y)e^{j\underline{k}\cdot\underline{r}}\,dk_x dk_y \quad (24a)$$

$$\hat{E}_y(x,y,z) = \frac{1}{4\pi^2}\int_{-\infty}^{\infty}\int_{-\infty}^{\infty}\hat{A}_y(k_x,k_y)e^{j\underline{k}\cdot\underline{r}}\,dk_x dk_y \quad (24b)$$

$$\hat{E}_z(x,y,z) = \frac{1}{4\pi^2}\int_{-\infty}^{\infty}\int_{-\infty}^{\infty}\hat{A}_z(k_x,k_y)e^{j\underline{k}\cdot\underline{r}}\,dk_x dk_y \quad (24c)$$

In a source-free region (which is the case with our near field measurements):

$$\nabla\cdot\hat{\underline{E}} = 0$$

where $\nabla = \underline{a}_x\frac{\partial}{\partial x} + \underline{a}_y\frac{\partial}{\partial y} + \underline{a}_z\frac{\partial}{\partial z}$.

Therefore in rectangular coordinates we have

$$\frac{\partial E_x(x,y,z)}{\partial x} + \frac{\partial E_y(x,y,z)}{\partial y} + \frac{\partial E_z(x,y,z)}{\partial z} = 0 \quad (25)$$

Substituting into (25) for the components of $\hat{\underline{E}}$ in terms of those for $\hat{\underline{A}}$ as given by (24) yields

$$\frac{1}{4\pi^2}\int_{-\infty}^{\infty}\int_{-\infty}^{\infty}\hat{A}_x(k_x,k_y)\frac{\partial}{\partial x}\left[e^{j(k_x x + k_y y + k_z z)}\right]dk_x dk_y$$

$$+ \frac{1}{4\pi^2}\int_{-\infty}^{\infty}\int_{-\infty}^{\infty}\hat{A}_y(k_x,k_y)\frac{\partial}{\partial y}\left[e^{j(k_x x + k_y y + k_z z)}\right]dk_x dk_y$$

$$+ \frac{1}{4\pi^2}\int_{-\infty}^{\infty}\int_{-\infty}^{\infty}\hat{A}_z(k_x,k_y)\frac{\partial}{\partial z}\left[e^{j(k_x x + k_y y + k_z z)}\right]dk_x dk_y = 0, \quad (26)$$

which, upon performing the partial diffenentiations, becomes

$$\frac{1}{4\pi^2}\int_{-\infty}^{\infty}\int_{-\infty}^{\infty}\left[jk_x\hat{A}_x(k_x,k_y) + jk_y\hat{A}_y(k_x,k_y)\right.$$

$$\left. + jk_z\hat{A}_z(k_x,k_y)\right]e^{j(k_x x + k_y y + k_z z)}\,dk_x dk_y = 0 \quad (27)$$

Cancelling out the j's in (27) and defining the resulting expression as $\hat{f}(x,y,z)$ gives us

$$\hat{f}(x,y,z) = \frac{1}{4\pi^2}\int_{-\infty}^{\infty}\int_{-\infty}^{\infty}\left[\underline{k}\cdot\hat{\underline{A}}\,(k_x,k_y)e^{jk_z z}\right]$$

$$e^{j(k_x x + k_y y)}\,dk_x dk_y = 0. \quad (28)$$

Because of the uniqueness of Fourier transform pairs,

$$\underline{k}\cdot\hat{\underline{A}}(k_x,k_y)e^{jk_z z} = \int_{-\infty}^{\infty}\int_{-\infty}^{\infty}\hat{f}(x,y,z)e^{-j(k_x x + k_y y)}\,dxdy. \quad (29)$$

But from (28),

$$\hat{f}(x,y,z) = 0$$

Therefore

$$\underline{k}\cdot\hat{\underline{A}}(k_x,k_y)e^{jk_z z} = 0 \text{ for all } z. \quad (30)$$

But $e^{jk_z z}$ is in general not equal to zero for all z. Therefore in order for (30) to be true for any z, we have the result that in a source-free region

$$\underline{k}\cdot\hat{\underline{A}} = 0. \quad (31)$$

This means that

$$k_x \hat{A}_x + k_y \hat{A}_y + k_z \hat{A}_z = 0 \tag{32}$$

from which we get

$$\hat{A}_z = -\frac{1}{k_z}\left[k_z \hat{A}_x + k_y \hat{A}_y\right] \tag{33}$$

where $k_z = \sqrt{k^2 - k_x^2 - k_y^2}$

and where (using (19)):

$$\hat{A}_x = \int_{-\infty}^{\infty}\int_{-\infty}^{\infty} E_x e^{-j\underline{k}\cdot\underline{r}} dxdy$$

$$= e^{-jk_z z_o} \int_{-\infty}^{\infty}\int_{-\infty}^{\infty} \hat{E}_x(x,y,z_o) e^{-j(k_x x + k_y y)} dxdy \tag{34a}$$

$$\hat{A}_y = \int_{-\infty}^{\infty}\int_{-\infty}^{\infty} \hat{E}_y e^{-j\underline{k}\cdot\underline{r}} dxdy$$

$$= e^{-jk_z z_o}\int_{-\infty}^{\infty}\int_{-\infty}^{\infty} \hat{E}_y(x,y,z_o) e^{-j(k_x x + k_y y)} dxdy \tag{34b}$$

The key result is that since, from (33), $\hat{A}_z$ is a function of $\hat{A}_x$ and $\hat{A}_y$, measurement is only required of the x and y components of $\underline{\hat{E}}$ to get $\underline{\hat{A}}$. Stated in more general terms, only two measurements of $\underline{\hat{E}}$, each taken at different orientations of the measurement antenna, are required to obtain all of the components of $\underline{\hat{A}}$.

The vector fields, $\hat{\underline{A}}$ and $\hat{\underline{E}}$, can also be expressed in spherical coordinates as

$$\hat{\underline{A}} = \underline{a}_r \hat{A}_r + \underline{a}_\theta \hat{A}_\theta + \underline{a}_\phi \hat{A}_\phi \qquad (35a)$$

and

$$\hat{\underline{E}} = \underline{a}_r \hat{E}_r + a_\theta \hat{E}_\theta + \underline{a}_\phi \hat{E}_\phi \qquad (35b)$$

where $\underline{a}_r$, $\underline{a}_\theta$, $\underline{a}_\phi$, are the unit direction vectors. In the far field of an antenna the radial component of the electric field, $\hat{E}_r$, is negligible compared to the other components. Thus in the far field

$$\hat{E} \tilde{=} \underline{a}_\theta \hat{E}_\theta + \underline{a}_\phi \hat{E}_\phi . \qquad (36)$$

2.6 Far Field Solution Using Method of Stationary Phase

The far field solution for the electric field, $\hat{\underline{E}}$, in (19b) is obtained below after R. Collin[11] using the method of "Stationary Phase".

The geometry of the situtation is depicted by the coordinates diagram in Figure 2. In rectangular coordinates,

$$\underline{r} = x\underline{a}_x + y\underline{a}_z + z\underline{a}_z . \qquad (37)$$

It is easy to show from Figure 2 that the x,y,z components of $\underline{r}$ are given in terms of the spherical coordinates, r, θ, and ϕ as

$$x = r \sin\theta \cos\phi \tag{38a}$$

$$y = r \sin\theta \sin\phi \tag{38b}$$

$$z = r \cos\theta \tag{38c}$$

Since

$$\underline{k} = k_x\underline{a}_x + k_y\underline{a}_y + k_z\underline{a}_z,$$

then the "phase" term $\underline{k} \cdot \underline{r}$ in (19b) becomes

$$\underline{k} \cdot \underline{r} = k_x x + k_y y + k_z z$$

$$= (k_x \sin\theta \cos\phi + k_y \sin\theta \sin\phi + k_z \cos\theta) r \tag{39}$$

where $k_z = \sqrt{k^2 - k_x^2 - k_y^2}$. Using the Euler identity, we can also express the term $e^{j\underline{k} \cdot \underline{r}}$ in (19b) as

$$e^{j\underline{k} \cdot \underline{r}} = \cos(\underline{k} \cdot \underline{r}) + j \sin(\underline{k} \cdot \underline{r}).$$

The "phase" term $\underline{k} \cdot \underline{r}$ is in general composed of real and imaginary parts, since k_z, in (39), can be real or imaginary as seen from (20). Thus letting $\underline{k} \cdot \underline{r}$ be described by

$$j\underline{k} \cdot \underline{r} = -\gamma' r = -(\alpha' + j\beta')r,$$

where α' and β' are real numbers (attenuation and phase constants, respectively), we then get

$$e^{j\underline{k} \cdot \underline{r}} = e^{-\alpha' r} e^{-j\beta' r}$$

$$= e^{-\alpha' r}(\cos\beta' r + j \sin\beta' r). \tag{40}$$

When r is very large, we see from (40) that the real and imaginary components of $e^{j\underline{k} \cdot \underline{r}}$ oscillate very rapidly between equal positive and negative values except for certain values of k_x and k_y for which $\underline{k} \cdot \underline{r}$ doesn't change much for changes in k_x and k_y. For those values of k_x and k_y the first order change in $\underline{k} \cdot \underline{r}$ is zero for small changes in k_x and k_y. Conversely $\hat{\underline{A}}(k_x,k_y)$ in (19b) is a slowly varying function in k_x and k_y (as compared with $\underline{k} \cdot \underline{r}$ being a rapidly varying function in k_x and k_y). Thus the contribution to the value of the integrals over all k_x and k_y of $\hat{\underline{A}}$ multiplied by $e^{j\underline{k} \cdot \underline{r}}$ comes essentially only from the values of $\hat{\underline{A}}$ determined by the k_x and k_y which make the "phase", $\underline{k} \cdot \underline{r}$, "stationary" (constant). The "phase" is stationary when

$$\frac{\partial \underline{k} \cdot \underline{r}}{\partial k_x} = \frac{\partial \underline{k} \cdot \underline{r}}{\partial k_y} = 0 \tag{41}$$

Using the value for $\underline{k} \cdot \underline{r}$ from (39),

$$\frac{\partial \underline{k} \cdot \underline{r}}{\partial k_x} = \frac{\partial}{\partial k_x} (k_x \sin\theta \cos\phi + k_y \sin\theta \sin\phi$$

$$+ \sqrt{k^2 - k_x^2 - k_y^2} \cos\theta) r = 0.$$

$$= (\sin\theta \cos\phi - \frac{k_x \cos\theta}{k_z}) = 0.$$

Therefore

$$k_x = \frac{k_z \sin\theta \cos\phi}{\cos\theta} . \qquad (42)$$

Likewise, $\partial \underline{k} \cdot \underline{r} / \partial k_y$ yields

$$k_y = \frac{k_z \sin\theta \sin\phi}{\cos\theta} \qquad (43)$$

But

$$k_z^2 = k^2 - k_x^2 - k_y^2 ,$$

which upon substitution of the values of k_x and k_y into (42) and (43) gives

$$k_z^2 = k^2 - k_z^2 \frac{\sin^2\theta}{\cos^2\theta}$$

which yields

$$k_z = k \cos\theta . \qquad (44)$$

Combining the results of (44) with (42) and (43) yields k_{x_o}, k_{y_o}, k_{z_o}, which we will define as those value of k_x, k_y, k_z for which $\underline{k} \cdot \underline{r}$ is stationary, namely:

$$k_{z_o} = k \cos\vartheta \qquad (45a)$$

$$k_{x_o} = k \sin\theta \cos\phi \qquad (45b)$$

$$k_{y_o} = k \sin\theta \sin\phi \qquad (45c)$$

(Note from (45a) that $k_z = k_{z_o}$ is real and therefore $\alpha = 0$ in (21). Therefore we have non-evanescence.) The phase $\underline{k} \cdot \underline{r}$ can be expanded in a Taylor series about k_{x_o} and k_{y_o}:

$$\underline{k} \cdot \underline{r} = \underline{k} \cdot \underline{r} \Big|_{k_{x_o}, k_{y_o}} + \frac{\partial \underline{k} \cdot \underline{r}}{\partial k_x}\Big|_{k_{x_o}, k_{y_o}} \Delta k_x + \frac{\partial \underline{k} \cdot \underline{r}}{\partial k_y}\Big|_{k_{x_o}, k_{y_o}} \Delta k_y$$

$$+ \tfrac{1}{2} \frac{\partial^2 \underline{k} \cdot \underline{r}}{\partial k_x^2}\Big|_{k_{x_o}, k_{y_o}} \Delta k_x^2 + \frac{1}{2} \frac{\partial^2 \underline{k} \cdot \underline{r}}{k_y^2}\Big|_{k_{x_o}, k_{y_o}} \Delta k_y^2$$

$$+ \frac{\partial^2 \underline{k} \cdot \underline{r}}{\partial k_x \, \partial k_y}\Big|_{k_{x_o}, k_{y_o}} \Delta k_x \, k_y + \ldots . \qquad (46)$$

where

$$\Delta k_x \triangleq k_x - k_{x_o}$$

and

$$\Delta k_y \triangleq k_y - k_{y_o} .$$

But (41) tells us that

$$\frac{\partial \underline{k} \cdot \underline{r}}{\partial k_x}\Big|_{k_{x_o}, k_{y_o}} \equiv \frac{\partial \underline{k} \cdot \underline{r}}{\partial k_y}\Big|_{k_{x_o}, k_{y_o}} = 0,$$

and (39) and (45) give us

$$\underline{k} \cdot \underline{r}\Big|_{k_{x_o}, k_{y_o}} = (k_{x_o} \sin\theta \cos\phi + k_{y_o} \sin\theta \sin\phi + \sqrt{k^2 - k_{x_o}^2 - k_{y_o}^2} \cos\theta) r$$

$$= (k \sin^2\theta \cos^2\phi + k \sin^2\theta \sin^2\phi + k \cos^2\theta) r$$

$$= kr$$

Therefore, (46) becomes:

$$\underline{k} \cdot \underline{r} \cong kr + (a\Delta k_x^2 + b\Delta k_x \Delta k_y + c\Delta k_z^2) \qquad (47)$$

where

$$a = \tfrac{1}{2} \frac{\partial^2 \underline{k} \cdot \underline{r}}{\partial k_x^2}, \quad b = \frac{\partial^2 \underline{k} \cdot \underline{r}}{\partial k_x \partial k_y}, \quad c = \tfrac{1}{2} \frac{^2\underline{k} \cdot \underline{r}}{\partial k_y^2},$$

all evaluated at $k_x = k_{x_o}$ and $k_y = k_{y_o}$.

Therefore we have in (19b) that

$$\hat{\underline{E}}(r) \equiv \hat{\underline{E}}(x,y,z) \frac{1}{4\pi^2} \int_{-\infty}^{\infty}\int_{-\infty}^{\infty} \hat{\underline{A}}(k_x,k_y) e^{j\underline{k} \cdot \underline{r}} dk_x dk_y$$

$$= \frac{1}{4\pi^2}\int_{-\infty}^{\infty} \int_{-\infty}^{\infty} \hat{\underline{A}}(k_{x_o},k_{y_o}) e^{j(kr + a\Delta k_x^2 + b\Delta k_x \Delta k_y + c\Delta k_y^2)} dk_x dk_y$$

$$= \frac{1}{4\pi^2} \hat{\underline{A}}(k_{x_o},k_{y_o}) e^{jkr} \int_{-\infty}^{\infty}\int_{-\infty}^{\infty} e^{j(au^2 + buv + cu^2)} dudv \qquad (48)$$

where $u = \Delta k_x$ and $v = \Delta k_y$. It can be shown that the double integral of the exponential term in (48) evaluates to

$$\frac{2\pi}{\sqrt{b^2 - 4ac}} = j\frac{2\pi}{r} k_{z_o}. \qquad (49)$$

When r is very large, we are in the far field (subject to (1)). In the far field then, we have (from (48) and (49)):

$$\hat{\underline{E}}(\underline{r}) = j\frac{e^{jkr}}{2\pi r} k_{z_o} \hat{\underline{A}}(k_{x_o}, k_{y_o}) \qquad (50)$$

with $k_{x_o}, k_{y_o}, k_{z_o}$ given by (45). Using (23) we can express $\hat{\underline{A}}$ in (50) in an explicit manner to give the far field in terms of the near field:

$$\hat{\underline{E}}(\underline{r}) = j\frac{ke^{jkr}}{2\pi r} e^{jkz_o\cos\theta} \cos\theta$$

$$\cdot \int_{-\infty}^{\infty}\int_{-\infty}^{\infty} \hat{\underline{E}}(x,y,z_o) e^{-jk \sin\theta(x\cos\phi + y\sin\phi)} dxdy \qquad (51)$$

where, from (37) and (38),

$$\underline{r} = \underline{a}_x r \sin\theta\cos\phi + \underline{a}_y \sin\theta\sin\phi + \underline{a}_z r\cos\theta.$$

2.7 Probe Compensation

Although (51) describes the far field precisely in terms of the near field, in a practical sense it does not describe the far field in terms of near field measurements. The reason of course is that any measurement of the near field, plane wave or otherwise, is altered by the measure-

ment probe characteristics. So the near field in a plane, represented by $\hat{\underline{E}}(x,y,z_o)$ in (51), would have to be obtained by deconvolution from actual near field measurements. Alternately, the far field can be obtained directly in a form that uses the near field measurements, but in conjunction with a description of the probe antenna pattern such that compensation is made for the probe characteristics. Such is the form given in References 3 and 12 and derived below. (However the derivation here is different than that in Reference 3 where the Lorentz reciprocity theorem is used instead.)

Consider the geometry of the antenna and measurement system shown in Figure 4. For the moment, let the measurement

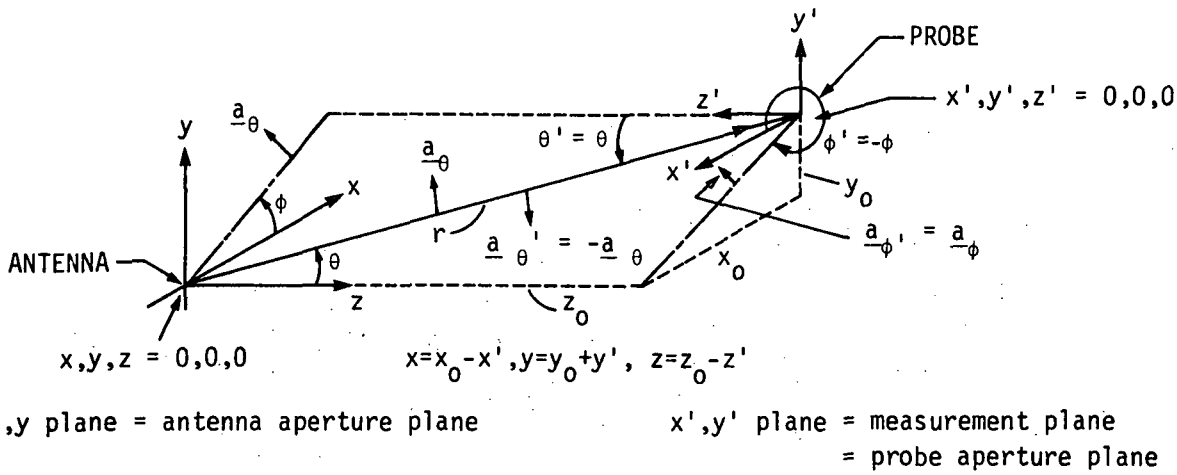

FIGURE 4

GEOMETRICAL RELATIONSHIP OF ANTENNA AND MEASUREMENT PROBE

system be an "infinitesimal" probe located at the coordinates $x_o, y_o z_o$ in the x,y,z coordinate system (0,0,0 in the x', y', z' system.) Let the probe's measurement characteristic be described by the vector/phasor term $\hat{\underline{C}} = \hat{c}dxdy$, where

$$\hat{\underline{c}} = \hat{\underline{c}}(x,y,z) = \hat{c}_1(x,y,z)\,\underline{a}_x + \hat{c}_2(x,y,z)\,\underline{a}_y + \hat{c}_3(x,y,z)\underline{a}_z. \tag{52}$$

When the probe is oriented so that it "points" in a direction perpendicular to the antenna aperture plane, we have $\hat{\underline{C}}' = \hat{c}'dx'dy'$, where

$$\hat{c}'(x',y',z') = \hat{c}_1(x',y',z')\underline{a}_{x'} + \hat{c}_2(x',y',z')\underline{a}_{y'} + \hat{c}_3(x',y',z')\underline{a}_{z'}, \tag{53}$$

But it can be shown from Figure 4 that the unit direction vectors and the differentials dx', dy' in the x', y', z' coordinate system are related to those in the x,y,z system as follows:

$$\underline{a}_{x'} = -\underline{a}_x$$

$$\underline{a}_{y'} = \underline{a}_y$$

$$\underline{a}_{z'} = -\underline{a}_z$$

$$dx' = -dx$$

$$dy' = dy$$

Therefore a voltage received by the "infitesimal" probe can be represented as

$$\begin{aligned}
\hat{dv}(x_o,y_o,z_o) &= [-\hat{E}_x(x_o,y_o,z_o)\hat{c}_1(0,0,0) \\
&\quad + \hat{E}_y(x_o,y_o,z_o)\hat{c}_2(0,0,0) \\
&\quad - \hat{E}_z(x_o,y_o,z_o)\hat{c}_3(0,0,0)]dxdy \\
&= [\hat{E}_x(x_o,y_o,z_o)\ \underline{a}_x + \hat{E}_y(x_o,y_o,z_o)\ \underline{a}_y \\
&\quad + \hat{E}_z(x_o,y_o,z_o)\underline{a}_z] \cdot [-\hat{c}_1(0,0,0)\ \underline{a}_x \\
&\quad + \hat{c}_2(0,0,0)\ \underline{a}_y - \hat{c}_3(0,0,0)\ \underline{a}_z]\ dxdy \\
&= [\hat{E}_x(x_o,y_o,z_o)\ \underline{a}_x + \hat{E}_y(x_o,y_o,z_o)\ \underline{a}_y \\
&\quad + \hat{E}_z(x_o,y_o,z_o)\underline{a}_z] \cdot [\hat{c}_1(0,0,0)\ \underline{a}_x \\
&\quad + \hat{c}_2(0,0,0)\underline{a}_y + \hat{c}_3(0,0,0)\ \underline{a}_z] \ (-dx')dy' \\
&= \underline{\hat{E}}(x_o,y_o,z_o) \cdot [-\underline{\hat{c}}'(0,0,0)]\ dx'dy'. \qquad (54)
\end{aligned}$$

Equation (54) becomes

$$\hat{dv}(x_o,y_o,z_o) = \underline{\hat{E}}(x,y,z) \cdot [-\underline{\hat{c}}'(x',y',z')]\ dx'dy'\Big|_{x'=y'=z'=0} \qquad (55)$$

where, from Figure 5,

$$x = x_o - x',\ y = y_o + y',\ z = z_o - z'. \qquad (56)$$

Thus from (55) and (56) we get

$$\hat{dv}(x_o,y_o,z_o)$$

$$= \hat{\underline{E}}(x_o - x',\ y_o + y',\ z_o - z') \cdot [-\hat{\underline{c}}'(x',y',z')]$$

$$dx'dy' \Big|_{x'=y'=z'=0} \quad (57)$$

Let a probe with an aperture area, $\mathcal{A}$, *be now placed about* the point 0,0,0 in the x',y' plane with the probe aperture parallel to the x,y plane, as shown in Figure 5. Let the

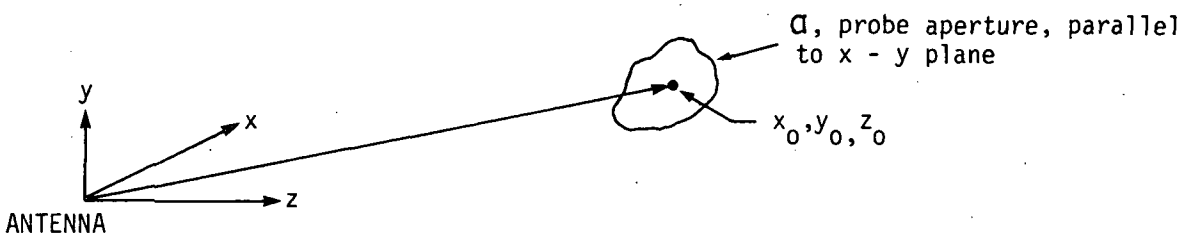

FIGURE 5

RELATIONSHIP OF PROBE APERTURE TO ANTENNA

probe aperture be filled with an infinite number of infinitesimal probe antennas which are described by (57). Let us further assume that each of the infinitesimal probe antennas responds equally to the same field (ie., uniform illumination taper for the probe aperture). Then from (57) the probe's response to the field $\hat{\underline{E}}$ is

$$\hat{v}(x_o,y_o,z_o) \triangleq \int d\hat{v}$$

$$= \int\int_{\mathcal{A}(0,0,0)} \hat{\underline{E}}(x_o - x',\ y_o + y',\ z_o - z') \cdot [-c'(x',y',z')]dx'dy' \Big|_{z'=0}$$

$$= \int\int_{\mathcal{A}} \hat{\underline{E}}(x_o - x',\ y_o + y',\ z_o) \cdot [-c'(x',y',o)]dx'dy' \quad (58)$$

If the probe aperture is not uniformly illuminated, then

$$\hat{v}(x_o,y_o,z_o) = \int_{\mathcal{A}}\int \hat{\underline{E}}(x_o - x',\ y_o + y',\ z_o)$$

$$\cdot\ [-\underline{c}'(x',y',o)f(x',y')]dx'dy' \quad (59)$$

where $f(x',y')$ is the illumination taper. In (59), let the term $\hat{\underline{g}}$ be defined such that

$$\hat{\underline{g}}(x',y') \triangleq -\hat{c}(x',y',o)f(x',y'). \quad (60)$$

Thus we see that $\hat{\underline{g}}$ is proportional to the aperture field distribution of the probe. Now the illumination taper, f, is zero outside $\mathcal{A}$. Therefore (59) can be expressed as

$$\hat{v}(x_o,y_o,z_o) =$$

$$\int_{-\infty}^{\infty}\int_{-\infty}^{\infty} \hat{\underline{E}}(x_o - x',\ y_o + y',\ z_o)$$

$$\cdot\ \hat{\underline{g}}(x',y')dx'dy'. \quad (61)$$

Let the probe aperture not be restricted to the location about x_o,y_o. Let it be free to move about in the measurement plane at $z = z_o$. Therefore in general, the measurement probe response in the measurement plane is

$$\hat{v}(x,y,z_o) = \int_{-\infty}^{\infty}\int_{-\infty}^{\infty} \hat{\underline{E}}(x - x',\ y + y',\ z_o) \cdot \hat{\underline{g}}(x',y')dx'dy'. \quad (62)$$

Let us examine the nature of the integrations performed in (62). To that end, let a variable, w, be the result

of the convolution of two other variables, u and v, such that

$$w(t) = \int_{-\infty}^{\infty} u(t - \tau)v(\tau)d\tau.$$

Therefore the Fourier transform of w, $\mathcal{F}\{w\}$, is given by

$$\mathcal{F}\{w\} = \mathcal{F}\{u\}\mathcal{F}\{v\}.$$

On the other hand let w be the result of the correlation of u and v such that

$$w(\tau) = \int_{-\infty}^{\infty} u(t + \tau)v(t)dt.$$

Therefore,

$$w(\tau) = \int_{-\infty}^{\infty} u(t)v(t - \tau)dt$$

$$= \int_{-\infty}^{\infty} u(t)v[-(\tau - t)]dt$$

so that the Fourier transform of w is

$$\mathcal{F}\{w(\tau)\} = \mathcal{F}\{u(\tau)\}\mathcal{F}\{v(-\tau)\}$$

$$= \mathcal{F}\{u(\tau)\}\ \mathcal{F}^*\{v(\tau)\}$$

where $\mathcal{F}^*$ is the complex conjugate of $\mathcal{F}$ such that

$$\mathcal{F}^*\{f(t)\} = F^*(jw) = F(-jw).$$

Therefore the two-dimensional Fourier transform of the voltage, $\hat{v}(x,y,z_o)$, measured by the probe in the near

field, where $\hat{v}$ is expressed by (62), can be expressed in terms of the two-dimensional Fourier transforms of $\underline{\hat{E}}$ and $\underline{\hat{g}}$ as

$$\int_{-\infty}^{\infty}\int_{-\infty}^{\infty} \hat{v}(x,y,z_o)e^{-j(k_x x + k_y y)}\,dxdy$$

$$= \int_{-\infty}^{\infty}\int_{-\infty}^{\infty} \underline{\hat{E}}(x,y,z_o)e^{-j(k_x x + k_y y)}\,dxdy$$

$$\cdot \int_{-\infty}^{\infty}\int_{-\infty}^{\infty} \underline{\hat{g}}(x,-y)e^{-j(k_x x + k_y y)}\,dxdy$$

$$= [\underline{\hat{A}}(k_x,k_y)e^{jk_z z_o}]\cdot \underline{\hat{G}}(k_x,-k_y) \qquad (63)$$

where the bracketed term is from (22). The term $\underline{\hat{G}}$ is equivalent to the far field radiation pattern of the probe. This is because the far field radiation pattern of an antenna results from the Fourier transform of the aperture field distribution which here is proportional to $\hat{g}$.

Multiplying both sides of (63) by the term

$$j\,\frac{e^{jkr}}{2\pi r}\,k_z$$

and evaluating the resulting expression at the modes given by (45):

$$k_x = k_{x_o} = k \sin\theta \cos\phi$$

$$k_y = k_{y_o} = k \sin\theta \sin\phi$$

$$k_z = k_{z_o} = k \cos\theta$$

yields

$$\left[j\frac{e^{jkr}}{2\pi r} k_{z_o} \hat{\underline{A}}(k_{x_o}, k_{y_o}) e^{jk_{z_o} z_o}\right] \cdot \hat{\underline{G}}(k_{x_o}, -k_{y_o})$$

$$= j\frac{e^{jkr}}{2\pi r} k_{z_o} \int_{-\infty}^{\infty}\int_{-\infty}^{\infty} v(x,y,z_o) e^{-j(k_{x_o} x + k_{y_o} y)} \, dxdy. \quad (64)$$

Upon substituting the result of (50) into (64) we get

$$\underline{E}(\underline{r}) \cdot \underline{G}(k_{x_o}, -k_{y_o})$$

$$= jk_{z_o} \frac{e^{jkr}}{2\pi r} e^{-jk_{z_o} z_o} \cdot \int_{-\infty}^{\infty}\int_{-\infty}^{\infty} v(x,y,z_o) e^{-j(k_{x_o} x + k_{y_o} y)} \, dxdy. \quad (65)$$

It is helpful to express this result in terms of spherical coordinates:

$$\hat{\underline{E}}(\underline{r})\Big|_{\text{far field}} = \hat{E}_r(r,\theta,\phi)\underline{a}_r + E(r,\theta,\phi)\underline{a}_\theta + \hat{E}_\phi(r,\theta,\phi)\underline{a}_\phi.$$

But the radial component of an electric field in the far field of an antenna is, for practical purposes, zero. Therefore,

$$\hat{E}_r(r,\theta,\phi) = 0 .$$

The shape of the other components of the electric field, $\hat{E}_\theta$ and $\hat{E}_\phi$ are independent of the distance, r, to the antenna (by definition of the far field). Thus without loss in generality we can write

$$\hat{\underline{E}}(r)\Big|_{\text{far field}} = E_\theta(\theta,\phi)\underline{a}_\theta + E_\phi(\theta,\phi)\ \underline{a}_\phi . \quad (66)$$

Likewise for $\underline{G}$ in spherical coordinates:

$$\hat{\underline{G}}(k_{x_o},-k_{y_o})$$

$$= \hat{\underline{G}}(k \sin\theta \cos\phi, - k \sin\theta \sin\phi)$$

$$= \underline{G}(k \sin\theta \cos(-\phi), k \sin\theta \sin(-\phi)).$$

We see from Figure 5 that

$$\phi' = -\phi, \ \theta' = \theta. \quad (67)$$

Therefore

$$\hat{\underline{G}}(k_{x_o}, -k_{y_o}) = \hat{\underline{G}}(k \sin\theta' \cos\phi', k \sin\theta' \sin\phi'). \quad (68)$$

The far field radiation pattern, $\hat{\underline{G}}$, can then be rewritten as $\underline{G}(\theta',\phi')$ which can be expanded in spherical coordinates as

$$\hat{\underline{G}}(\theta',\phi') = \hat{G}_\theta(\theta',\phi')\underline{a}_\theta' + \hat{G}_\phi(\theta',\phi')\underline{a}_\phi'$$

$$+ \hat{G}_r(\theta',\phi')\underline{a}_r'. \quad (69)$$

Since the radial component of the electric field transmitted by an antenna is effectively zero in the far field, by reciprocity the radial component of an antenna's far field receiving pattern is zero. Therefore in (69),

$$\hat{G}_r(\theta',\phi') = 0. \tag{70}$$

Adding this to the fact that from Figure 4

$$a_\theta' = -a_\theta,\ a_\phi' = a_\phi'. \tag{71}$$

Equation (69), with the use of (67), becomes

$$\underline{\hat{G}} = -\hat{G}_\theta(\theta,-\phi)\underline{a}_\theta + \hat{G}_\phi(\theta,-\phi)\underline{a}_\phi .$$

Therefore the expression in (65) can be evaluated in terms of the angles θ and ϕ to give us the relationship between the far field pattern of an antenna and the far field radiation pattern of a measurement probe. The relationship is given in terms of the spatial Fourier transform of the voltage measured by the probe in the antenna's near field and the vector components of $\underline{\hat{E}}$ and $\underline{\hat{G}}$:

$$-\hat{E}_\theta(\theta,\phi)\hat{G}_\theta(\theta,-\phi) + \hat{E}_\phi(\theta,\phi)\hat{G}_\phi(\theta,-\phi)$$

$$= j\frac{ke^{jkr}}{2\pi r} e^{-jkz_o\cos\theta} \cos\theta \int_{-\infty}^{\infty}\int_{-\infty}^{\infty}$$

$$\hat{v}(x,y,z_o)e^{-jk\sin\theta(x\cos\phi + y\sin\theta)}dxdy. \tag{72}$$

The probe measurement will in practice be a set of discrete samples. The double integration in (72) then becomes a double summation discrete approximation which can be efficiently evaluated using the Fast Fourier Transform.

Equation (72) expresses the far field radiation pattern of the antenna's electric field in terms of the two orthogonal field components, $\hat{E}_\theta$, and $\hat{E}_\phi$. The terms $\hat{G}_\theta$ and $\hat{G}_\phi$ are the two known (orthogonal) components of the far field radiation of the probe. They are expressed in the direction $(\theta, -\phi)$ from the probe to the phase center of the antenna (which is opposite to the direction (θ,ϕ) from the antenna to the probe.) Thus we have one (linear) equation and two unknowns. Therefore a second, linearly independent equation is needed to solve for the two unknowns ($\hat{E}_\theta$ and $\hat{E}_\phi$). A rotation of the probe, which thereby changes the polarization axis (axes), provides the needed second equation. The second equation has the form

$$- \hat{E}_\theta(\theta,\phi)\hat{G}_{R\theta}(\theta,-\phi) + \hat{E}_\phi(\theta,\phi)\hat{G}_{R\theta}(\theta,-\phi)$$

$$= j\frac{ke^{jkr}}{2\pi r} e^{-jkz_o\cos\theta} \cos\theta \int_{-\infty}^{\infty}\int_{-\infty}^{\infty}$$

$$\hat{v}_R(x,y,z_o)e^{-jk\sin\theta(x\cos\phi + y\sin\phi)}dxdy \quad (73)$$

where the subscript, R, refers to quantities resulting from the probe rotation.

Therefore for each θ, ϕ combination we have two independent equations for the two unknowns, $\hat{E}_\theta$ and $\hat{E}_\phi$:

$$-\hat{E}_\theta \hat{G}_\theta + \hat{E}_\phi \hat{G}_\phi = \text{result of measurement \#1}$$

$$-\hat{E}_\theta \hat{G}_{R\theta} + \hat{E}_\theta \hat{G}_{R\phi} = \text{result of measurement \#2}.$$

These two equations immediately above are solvable if the determinant

$$\nabla = \begin{vmatrix} \hat{G}_\theta & \hat{G}_\phi \\ \hat{G}_{R\theta} & \hat{G}_{R\phi} \end{vmatrix} = \hat{G}_\theta \hat{G}_{R\phi} - \hat{G}_\phi \hat{G}_{R\theta} \neq 0$$

(The determinant will be zero for the case where the probe is circularly polarized because such a probe will obviously give no new information upon rotation.)

2.8 Other Modal Expansions

Our focus in the report has been the plane wave modal expansion - antenna patterns from measurements made over a planar surface. Far field antenna patterns can also be obtained from measurements made over cylindrical[9] and spherical surfaces[1] (Figure 6). These surfaces arise as a natural consequence of the type of probe scanning employed, as does the planar. The cylindrical results from vertical scanning of the probe together with rotation is azimuth of the antenna under test.

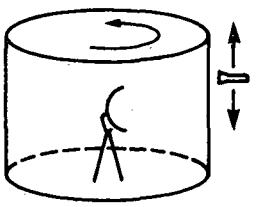

CYLINDRICAL-WAVE MODAL EXPANSION

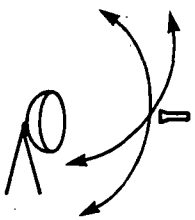

SPHERICAL-WAVE MODAL EXPANSION

FIGURE 6

OTHER MODAL EXPANSION MEASUREMENT SURFACES

Spherical is employed by fixing the probe in space and rotating the antenna in azimuth and elevation. This results in simpler probe calibration. These scanning surfaces naturally give rise respectively to cylindrical-wave and spherical-wave modal expansions. The Fast Fourier Transform can still be used for the cylindrical-wave modal expansion, however it cannot be used for the spherical-wave[1]. The spherical-wave modal expansion is computationally the most complicated.

3.0 Acoustic Waves

Let us now direct our attention to acoustic waves. Consider the acoustic wave equation for the instantaneous pressure increment, p:

$$\nabla^2 p = \frac{1}{c_a^2} \frac{\partial^2 p}{\partial t^2}$$

where ∇^2 is again the Laplacian, and c_a is the velocity of sound in air (for the sonic simulator). For a "monochromatic" (i.e., single tone) field,

$$p = \text{Real } \{\hat{p} e^{j\omega t}\}$$

and therefore,

$$\nabla^2 p = -\left(\frac{\omega}{c_a}\right)^2 \hat{p} \qquad (74a)$$

$$= -k^2 \hat{p} \qquad (74b)$$

where

$$k = \frac{\omega}{c_a} = \frac{2\pi}{\lambda_a}$$

and λ_a is the wavelength in air for a given radian frequency, $\omega = 2\pi f$. In rectangular coordinates,

$$\hat{p} = \hat{p}(x,y,z),$$

and, of course,

$$\nabla^2 = \frac{\partial^2}{\partial x^2} + \frac{\partial^2}{\partial y^2} + \frac{\partial^2}{\partial z^2} .$$

Taking the two-dimensional Fourier transform of the wave equation (74) with respect to x and y yields:

$$\int_{-\infty}^{\infty}\int_{-\infty}^{\infty} \nabla^2\hat{p}(x,y,z)e^{-j(k_x x + k_y y)}\,dxdy$$

$$= -k^2\hat{B}(k_x,k_y,z) \qquad (75)$$

where

$$\hat{B}(k_x,k_y,z) = \int_{-\infty}^{\infty}\int_{-\infty}^{\infty} \hat{p}(x,y,z)e^{-j(k_x x + k_y y)}\,dxdy. \qquad (76)$$

Note the similarity between (75), (76) and (7), (8). We see that the development here is identical to that of the electromagnetic case except that vectors such as $\underline{\hat{E}}$, $\underline{\hat{B}}$, and $\underline{\hat{A}}$ are replaced respectively with scalars such as

$\hat{p}$, $\hat{B}$, and $\hat{A}$. Thus we obviously obtain the results below for the acoustic case. In the far field, then,

$$\hat{p}(\underline{r}) = j\frac{e^{jkr}}{2\pi r} k_{z_o} \hat{A}(k_{x_o}, k_{y_o}) \tag{77}$$

where

$$\hat{A}(k_{x_o}, k_{y_o}) = e^{-jk_{z_o} z_o} \int_{-\infty}^{\infty}\int_{-\infty}^{\infty} \hat{p}(x,y,z_o) e^{-j(k_{x_o} x + k_{y_o} y)} dxdy \tag{78}$$

and where

$$k_{x_o} = k \sin\theta \cos\phi \tag{79a}$$

$$k_{y_o} = k \sin\theta \sin\phi$$

$$k_{z_o} = \sqrt{k^2 - k_{x_o}^2 - k_{y_o}^2} = k \cos\theta. \tag{79b}$$

Probe compensation then yields

$$\hat{A}(k_{x_o}, k_{y_o}) e^{jk_{z_o} z_o} \hat{G}(k_{x_o}, -k_{y_o})$$

$$= \int_{-\infty}^{\infty}\int_{-\infty}^{\infty} \hat{v}(x,y,z_o) e^{-j(k_{x_o} x + k_{y_o} y)} dxdy. \tag{80}$$

Multiplying both sides of (80) by the term

$$j \frac{e^{jkr}}{2\pi r} k_{z_o}$$

and then rearranging terms gives

$$\hat{p}(\underline{r})\hat{G}(k_{x_o},-k_{y_o}) = j\frac{e^{jkr}}{2\pi r} e^{-jk_{z_o}z_o} k_{z_o}$$

$$\cdot \int_{-\infty}^{\infty}\int_{-\infty}^{\infty} \hat{v}(x,y,z_o) e^{-j(k_{x_o}x + k_{y_o}y)} dxdy \quad (81)$$

which then becomes

$$\hat{p}(\theta,\phi)\hat{G}(\theta,-\phi) = j\frac{ke^{jkr}}{2\pi r} e^{-jkz_o\cos\theta} \cos\theta$$

$$\cdot \int_{-\infty}^{\infty}\int_{-\infty}^{\infty} \hat{v}(x,y,z_o) e^{-jk \sin\theta(x\cos\phi + y\sin\phi)} dxdy. \quad (82)$$

Note that (82) is identical to (72) with the exception of course that $\hat{p}$ and $\hat{G}$ are scalars instead of vectors $\hat{\underline{E}}$ and $\hat{\underline{G}}$. If we have chosen our coordinate system such that the z axis was parallel to one of the axes of polarization of the antenna instead of perpendicular as in Figures 2 and 3, we would get an equation in $E_\theta G_\theta$ and $E_\theta G_\theta$ similar to (72) and expressed in the resultant newly defined θ and ϕ[1]. However now the electric field in any plane where ϕ is constant would be due only to that one particular polarization. The electric field perpendicular to that plane would be due only to the other orthogonal polarization component. This means that for linear polarization in a direction parallel to the new z axis, E_ϕ would be zero in our new equation that is equivalent to (72). Since any electromagnetic wave can be decomposed into two orthogonal linear polarizations, the polarization component

perpendicular to the first would result in an E_ϕ - only component ($\hat{E}_\theta = 0$) in our new equation equivalent to (72). Thus our newly defined $\hat{E}_\theta$ and $\hat{E}_\phi$ are separable by polarization. Therefore acoustic simulation of electromagnetic waves can be performed wherein the new θ represents one polarization and the new ϕ the other. The sonically obtained voltage, $\hat{v}$, in (82) simulates the electromagnetically obtained voltage, $\hat{v}$, in our new equation equivalent to (72). (The simulation would be actually performed as two separate simulations, one for each polarization. The results of the two simulations would then be orthogonally superimposed to obtain the final result.)

4.0 Conclusions

(1) We see that near field to far field transformations are valid to obtain far field antenna information from near field measurements.

(2) Acoustic simulation of electromagnetic near field to far field transformations is valid.

(3) Polarization is easily accommodated acoustically* in the simulation of electromagnetic waves (including near field to far field transformations.)

*except for certain types of reflections external to the antenna.

SECTION II

MULTIPLE BEAM FORMING AND STEERING

1.0 Introduction

1.1 Background

Simulation software has been developed for the Retrodirective Phase Control Sonic Simulator to form and steer up to five sonic beams simultaneously and independently[14]. Two methods of beamforming and steering were investigated. One was retrodirective phase control and the other was a mathematically synthesized open loop phase control.

1.2 Beamforming with Sonic Simulator

Beamforming requires that the proper array amplitude and phase tapers be generated to form the beam(s) at the desired focal point(s). These tapers dictate the amplitude and phase of each array transmitting element's output. Beamforming can be though of as a two-step process:

Step #1. For each beam, determine for each transmitting element or group of elements the difference in two propagation phase delays. One phase delay is that between the beam focal point and an array reference point (near the center of the array.) The other delay is that between the beam focal point and the transmitting element

or group of transmitting elements. This process step can be called "phase tuning".

Retrodirective Phase Control - In this mode, the Sonic Simulator's transmitting elements are grouped together four-each in subarrays. The propagation phase delay difference in the Sonic Simulator system is measured directly as the phase difference between the pilot beam signal as received at the reference receiver on the array and as received at the center of each subarray. The focal point of the beam subsequently transmitted by the array is determined by the focal point of the pilot beam source.

Mathematically Synthesized Open Loop Phase Control - The phase taper is mathematically synthesized in this mode. The propagation phase delay difference is computed from the geometric difference in the path lengths, in wavelengths, to the beam focal point from the center of the array and from each transmitting element. It is easy to show that if, relative to the center of the array, the coordinates of the beam focal point are desired to be at (X,Y,Z), and if those of a transmitting element

are at (x,y), then the propagation phase delay difference is

$$\sqrt{x^2 + y^2 + z^2} = \sqrt{(x - x)^2 + (Y - y)^2 + z^2} \div \lambda \cdot 360^{\circ},$$

where λ is the wavelength.

Step #2. Determine the phase and amplitude (or power) of the output of each array transmitting element. The multiple beam forming method used with the Sonic Simulator enables all transmitting elements to contribute to all beams. The phase taper and amplitude taper required to form each beam separately are first determined. Then the resulting phase taper and amplitude taper required to transmit all beams simultaneously are obtained by superposition -- the phasor (vector) sum at each transmitting element of the phase and amplitude of its output which would be required to form each beam singly. This procedure is mechanized in the Sonic Simulator system for beams of equal power and shape by calculating each transmitting element's output phase and power (which is proportional to the square of its amplitude) according to Equations (58) and (59) and Appendix D in Reference 14:

PAGE 50 INTENTIONALLY BLANK

$$\Delta\phi_c = -\tan^{-1} \frac{\sum_{n=1}^{N} \sin\Delta\phi_{an}}{\sum_{n=1}^{N} \cos\Delta\phi_{an}} .$$

$$P_{T_N} = \alpha|F(r)|^2\left[\left(\sum_{n=1}^{N} \cos\Delta\phi_{an}\right)^2 + \left(\sum_{n=1}^{N} \sin\Delta\phi_{an}\right)^2\right].$$

where

$\Delta\phi_c$ = output phase of signal at transmitting element.

N = number of beams.

$\Delta\phi_{an}$ = the phases measured in Step #1 above.

P_{T_N} = output power of signal at transmitting element.

$\alpha|F(r)|^2$ = power taper as a function of radial distance, r, from center of array.

(Although the above phase and power equations were developed for the method of closed loop phase control[15], they are also valid for retrodirective and mathematical open loop phase control.)

The amplitude (power) taper used in the experiments run with the simulator is a 10 dB four-step approximation

to a gaussian curve. The step sizes are 2.5 dB. This is the amount by which the simulator's array is designed to vary the transmitting element's output power levels.

The program listing for the software used in the Sonic Simulator, including that for multiple beam forming, is given in 3.0 of Section II. The operation of the software is given in Reference 16.

2.0 Experimental Results

In the final analysis, the demonstration and evaluation of retrodirective and mathematically synthesized open loop phase control techniques for multiple simultaneous beam generation with a phased array antenna is proven by the actual generation of those beams. This is easily done using the Retrodirective Sonic Simulator to generate the beams and then making experimental investigations with the Beam/Pattern Monitor and Display System. The resulting multibeam data that is taken with the monitor can then be used to evaluate each technique against standard antenna performance criteria and to evaluate each technique against the other to determine their relative performance.

Figures 7 and 8 show far field patterns of multiple beams transmitted by the simulator array. The beams were focused in a plane 2.5 meters from the array.

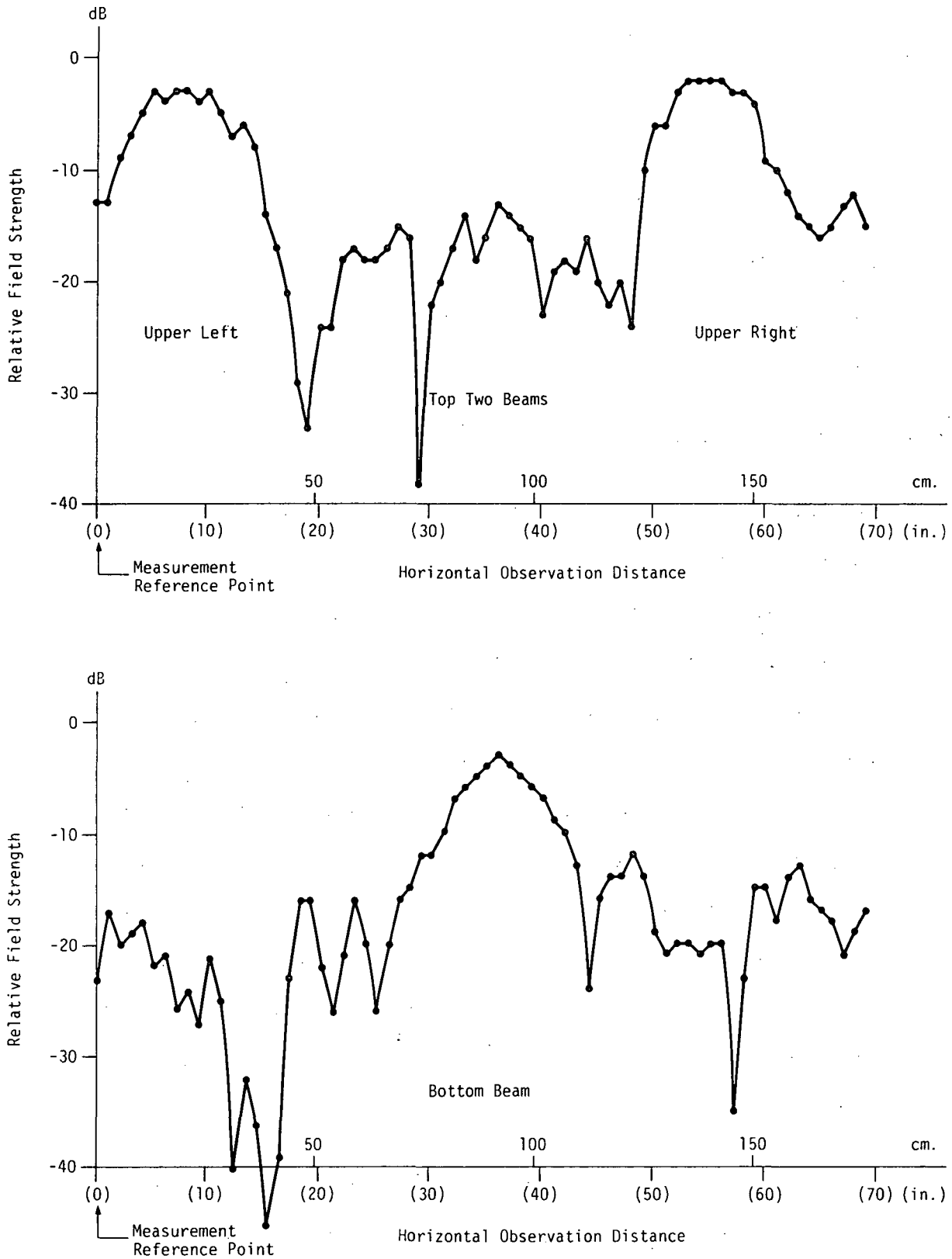

FIGURE 7

TRIPLE-BEAM FAR FIELD PATTERNS -- RETRODIRECTIVE PHASE CONTROL

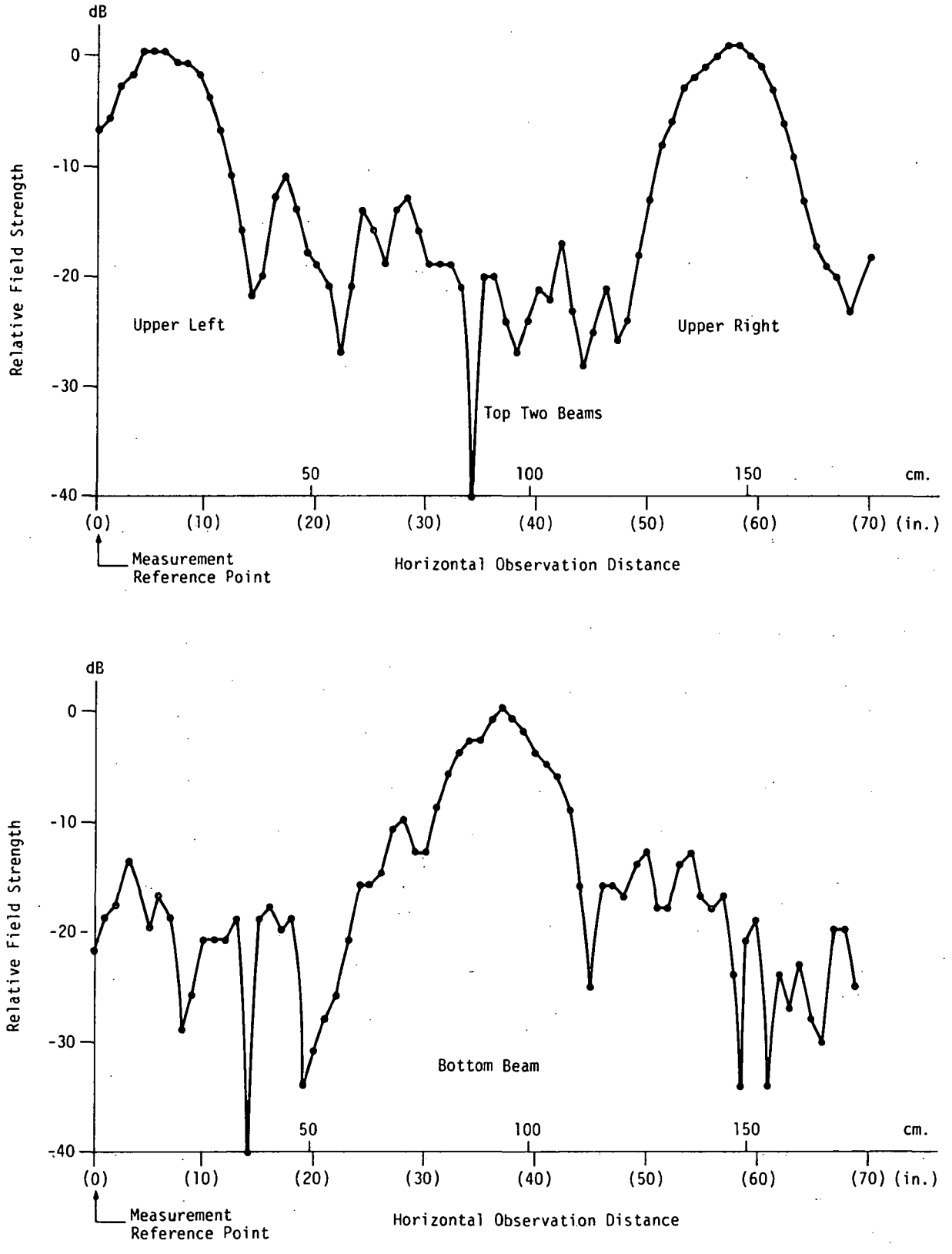

FIGURE 8

TRIPLE-BEAM FAR FIELD PATTERNS -- MATHEMATICAL OPEN LOOP PHASE CONTROL

("Left" and "right" in the figures are as viewed from the array.) The patterns are horizontal cuts made through the center of the beams in the focal plane. Each multibeam consists of three equal-power 10 dB truncated-gaussian amplitude taper beams. The top two beams were formed on centers about 1 m. apart and the bottom beam's center is about 0.8 m from the top two. The beams in Figure 7 were formed using retrodirective phase control and those in Figure 8 using mathematical open loop.

Although the sidelobes of the beams are higher than would be expected in free space, they are quite good and are to be expected for two reasons. For the sake of convenience, the measurements were made in a semi-anechoic environment. Secondly, the three beams in each multibeam were formed within several beamwidths of each other. The sidelobes of each individual beam are still of sufficient amplitude within that distance that at locations of phase reinforcement from two or more of the beams the resulting amplitude level can be much higher than that of a single sidelobe by itself.

The mathematically formed beams are seen to be more sharply defined than the retrodirective ones with about 3 dB higher amplitude and overall lower sidelobes. This is because for the sake of convenience the retro-directive beams were formed very close to the array

making it difficult to accurately illuminate the array with the retrodirective pilot signal. On the other hand, the mathematically formed beams were not as accurately pointed. A mathematically formed beam cannot track a receiver unless it has accurate information about the receiver location from another source.

3.0 Source Code Listing - Simulation Software

The following is the program listing, in BASIC, of the simulation software for the Retrodirective Sonic Simulator.

```
SIMULATOR DISK 1

10 OUT 2,15:OUT 2,7:OUT 3,79:OUT 3,7:OUT 0,255:OUT 0,5:OUT 0,4
20 DIM AY%(31,31,5)
30 DIM Y(4)
40 DIM SS(31,31,1)
50 CLOSE #1:PRINT CHR$(27);CHR$(69)
60 PRINT CHR$(27);"G"
70 PRINT "PRINTER OPTION ";
80 IF PR=0 THEN PRINT"OFF":GOTO 100
90 PRINT "ON"
100 PRINT:PRINT"KEY     FUNCTION                    KEY     FUNCTION":PRINT
110 PRINT" 1 INITIALIZE ARRAY                13 MULTIBEAM CONSTRUCT"
120 PRINT" 2 SELECT/DESELECT PRINTER         14 LOAD MULTIBEAM AMP TAPER"
130 PRINT" 3 MPC MODE CALC                   15 DISPLAY MULTIBEAM AMP PLOT/PATTERN"
140 PRINT" 4 RPC MODE READ                   16 SAVE MULTIBEAM DATA"
150 PRINT" 5 IPC MODE READ                   17 GET MULTIBEAM DATA"
160 PRINT" 6 LOAD PHASE TAPER                18 IPC RETUNE"
170 PRINT" 7 LOAD GAUSS AMP TAPER                19 MULTIBEAM RECONSTRUCT"
180 PRINT" 8 LOAD UNIFORM AMP TAPER          20 BEAM PHASE SHIFT"
190 PRINT" 9 DISPLAY PHASE PLOT              21 RANDOM PHASE ERROR ADD"
200 PRINT"10 DISPLAY PHASE PATTERN           22 RANDOM POWER-UP/DOWN"
210 PRINT"11 SAVE PHASE DATA                 23 COLUMN POWER-UP/DOWN"
220 PRINT"12 GET PHASE DATA                  24 SET OUTPUT FREQUENCY"
230 PRINT"                                   25 SEND 8-BIT WORD"
250 INPUT N
260 IF N>25 OR N<=0 THEN 250
270 ON N GOTO 4700,1630,330,590,790,1060,1180,1300,2160,1420,2300,2350,2680,3820,3470,4800,4830,4070,4080,3930,2480,4090,4520,4440,1
660
280 '
290 '
300 M$=INKEY$:IF M$="M" THEN GOTO 50
310 GOTO 300
320 '
330 GOSUB 1730
340 GOSUB 1710
350 GOSUB 1720
360 GOSUB 1750
370 GOSUB 1820
380 GOSUB 1790
381 N=.04572:IF L=16 THEN N=2*N
382 XX=XX/N:YY=YY/N:D=D/N
383 FOR C=0 TO L-1
384 FOR R=0 TO L-1
385 Z$=INKEY$:IF Z$="A" THEN 290
386 XYZ=(XX^2+YY^2+D^2)^.5
387 IF L=16 THEN B=((7.5-R)^2+(C-7.5)^2)*.09:BB=((YY-7.5+R)^2+(XX-C+7.5)^2+D^2)^.5:GOTO 470
388 B=((15.5-R)^2+(C-15.5)^2)*.0225:BB=((YY-15.5+R)^2+(XX-C+15.5)^2+D^2)^.5
470 IF B=>5.9 THEN P=0:GOTO 510
480 W=(64*F/(.33528/N))*(BB-XYZ)
490 P=INT(64*(W/64-INT(W/64))+64+.1)
500 IF B=>5.9 THEN 540
510 IF L=16 THEN 530
520 AY%(C,R,AY)=P:GOTO 540
530 AY%(2*C,2*R,AY)=P:AY%(2*C+1,2*R,AY)=P:AY%(2*C,2*R+1,AY)=P:AY%(2*C+1,2*R+1,AY)=P
540 GOSUB 1870
550 NEXT R
560 NEXT C
570 GOTO 290
580 '
590 OUT 0,255:OUT 0,5
600 OUT 0,5
610 OUT 0,255:OUT 0,3:L=16
620 GOSUB 1790
630 FOR C=0 TO 15
640 FOR R=0 TO 15
650 B=((7.5-R)^2+(C-7.5)^2)*.09
660 IF B=>5.9 THEN P=0:GOTO 720
670 Z$=INKEY$:IF Z$="A" THEN 290
680 OUT 0,255:OUT 0,2:OUT 0,C:OUT 0,R
690 FOR DC=0 TO 50
700 NEXT DC
710 GOSUB 4300
720 AY%(2*C,2*R,AY)=P:AY%(2*C+1,2*R,AY)=P:AY%(2*C,2*R+1,AY)=P:AY%(2*C+1,2*R+1,AY)=P
730 GOSUB 1870
740 NEXT R
750 NEXT C
```

```
760 OUT 0,255:OUT 0,5:OUT 0,4
770 GOTO 290
780 '
790 JR=3
800 GOSUB 1750
810 GOSUB 1790
820 OUT 0,255:OUT 0,5:OUT 0,4*(F/2-1)+2:OUT 0,255:OUT 0,4:L=32
830 FOR C=0 TO 31
840 FOR R=0 TO 31
850 Z$=INKEY$:IF Z$="A" THEN 290
860 IF JR=19 THEN P=AY%(C,R,5):GOTO 880
870 P=0
880 IF P=0 THEN P=64
890 OUT 0,255:OUT 0,1:OUT 0,C:OUT 0,R:OUT 0,P
900 OUT 0,255:OUT 0,1:OUT 0,C:OUT 0,R
910 OUT 0,0
920 FOR DC=0 TO 100
930 NEXT DC
940 GOSUB 4300
950 OUT 0,255:OUT 0,1:OUT 0,C:OUT 0,R:OUT 0,15
960 B=((15.5-R)^2+(C-15.5)^2)*.0225
970 IF B=>5.9 THEN P=0
980 AY%(C,R,AY)=P
990 GOSUB 1870
1000 NEXT R
1010 NEXT C
1020 OUT 0,255:OUT 0,5:OUT 0,4*(F/2-1)
1030 IF JR=19 THEN 290
1040 GOTO 290
1050 '
1060 GOSUB 1790
1070 GOSUB 4680
1080 GOSUB 4870
1090 FOR C=0 TO 31
1100 FOR R=0 TO 31
1110 Z$=INKEY$:IF Z$="A" THEN 290
1120 P=AY%(C,R,AY):IF P=0 THEN P=64
1130 OUT 0,255:OUT 0,1:OUT 0,C:OUT 0,R:OUT 0,P
1140 NEXT R
1150 NEXT C
1160 '
1170 GOTO 50
1180 GOSUB 1770
1190 GOSUB 4870
1200 FOR C=0 TO 31
1210 FOR R=0 TO 31
1220 Z$=INKEY$:IF Z$="A" THEN 290
1230 GOSUB 2620:AA=M+A: IF AA>15 THEN AA=15
1240 OUT 0,255:OUT 0,1:OUT 0,C:OUT 0,R:OUT 0,AA
1250 NEXT R
1260 NEXT C
1270 GOSUB 2000
1280 GOTO 50
1290 '
1300 GOSUB 1770
1310 GOSUB 4870
1320 FOR C=0 TO 31
1330 FOR R=0 TO 31
1340 Z$=INKEY$:IF Z$="A" THEN 290
1350 OUT 0,255:OUT 0,1
1360 OUT 0,C:OUT 0,R:OUT 0,A
1370 NEXT R
1380 NEXT C
1390 GOSUB 2000
1400 GOTO 50
1410 '
1420 GOSUB 1790
1430 S$=" `a^^bwi*+=-.@#%"
1440 PRINT:PRINT:PRINT:PRINT:IF PR=0 THEN 1460
1450 LPRINT:LPRINT:LPRINT:LPRINT
1460 PRINT CHR$(27);"F":IF PR=0 THEN 1480
1470 LPRINT CHR$(27);"[j0m";
1480 FOR R=0 TO 31
1490 Z=0
1500 FOR C=0 TO 31
1510 Z$=INKEY$:IF Z$="A" THEN 290
```

```
1520 V=INT((AY%(C,R,AY)-64)/5.8+.5)+1:IF V<1 THEN V=1
1530 D$=MID$(S$,V,1):PRINT D$;D$;
1540 IF PR=0 THEN 1560
1550 LPRINT D$;D$;D$;
1560 NEXT C
1570 PRINT:IF PR=0 THEN 1590
1580 LPRINT:Z=Z+1:IF Z=1 THEN 1500
1590 NEXT R
1600 PRINT CHR$(27);"G":IF PR=0 THEN 290
1610 LPRINT CHR$(27);"[11m":GOTO 290
1620 '
1630 IF PR=0 THEN PR=1:GOTO 50
1640 PR=0:GOTO 50
1650 '
1660 INPUT "KEY DECIMAL VALUE [0 TO 255]: ";Z$:Z=VAL(Z$):IF Z$="M" THEN 50
1670 IF Z<256 AND Z=>0 AND Z=INT(Z) THEN 1690
1680 PRINT "WHAT?":GOTO 1660
1690 OUT 0,Z:PRINT "* ";Z:GOTO 1660
1700 '
1710 INPUT "HORZ COORD ";XX:RETURN
1720 INPUT "VERT COORD ";YY:RETURN
1730 INPUT "DIST COORD ";D:IF D>0 THEN RETURN
1740 GOTO 1730
1750 INPUT "FREQUENCY ";F:IF F=2 OR F=4 OR F=6 THEN RETURN
1760 GOTO 1750
1770 INPUT "AMPLITUDE ";A:IF 0<=A AND A<16 AND A=INT(A) THEN RETURN
1780 GOTO 1770
1790 INPUT "ARRAY FILE # ";AY:IF 0<=AY AND AY<6 AND AY=INT(AY) THEN 2040
1800 GOTO 1790
1810 LINE INPUT "ARRAY FILE ";AY$:RETURN
1820 INPUT "RESOLUTION 16 OR 32 ";L:IF L=16 OR L=32 THEN RETURN
1830 GOTO 1820
1840 INPUT "GAUSSIAN OR UNIFORM---G OR U ";T$:IF T$="G" OR T$="U" THEN RETURN
1850 GOTO 1840
1860 '
1870 PRP=P-64:IF PRP<0 THEN PRP=0
1880 PRINT USING "## ";C;R;PRP;
1890 IF PR=0 THEN 1910
1900 LPRINT USING "## ";C;R;PRP;
1910 IF B=>5.9 THEN 1960
1920 FOR S=0 TO P-64
1930 PRINT "*";
1940 IF PR=1 THEN LPRINT"*";
1950 NEXT S
1960 PRINT
1970 IF PR=1 THEN LPRINT
1980 RETURN
1990 '
2000 DATA 1,9,1,22,9,1,9,30,22,1,22,30,30,9,30,22
2010 FOR X=1 TO 8
2020 READ C,R:OUT 0,255:OUT 0,1:OUT 0,C:OUT 0,R:OUT 0,15:NEXT X
2030 RESTORE:RETURN
2040 D$="012345"
2050 AY$=MID$(D$,AY+1,1)
2060 RETURN
2070 RESET
2080 OPEN "O",1,AY$
2090 FOR R=0 TO 31
2100 FOR C=0 TO 31
2110 WRITE #1,AY%(C,R,AY)
2120 NEXT C
2130 NEXT R
2140 CLOSE #1
2150 RETURN
2160 GOSUB 1790
2170 GOSUB 1820
2180 FOR C=0 TO L-1
2190 FOR R=0 TO L-1
2200 Z$=INKEY$:IF Z$="A" THEN 290
2210 IF L=16 THEN B=((7.5-R)^2+(C-7.5)^2)*.09:GOTO 2230
2220 B=((15.5-R)^2+(C-15.5)^2)*.0225
2230 IF L=16 THEN P=AY%(2*C,2*R,AY):GOTO 2250
2240 P=AY%(C,R,AY)
2250 IF P<64 THEN P=64
2260 GOSUB 1870
2270 NEXT R
2280 NEXT C
```

```
2290 GOTO 290
2300 PRINT "SOURCE ";:GOSUB 1790
2310 PRINT "DESTINATION ";:GOSUB 1810
2320 GOSUB 4870
2330 GOSUB 2070
2340 GOTO 50
2350 PRINT "DESTINATION ";:GOSUB 1790
2360 PRINT "SOURCE ";:GOSUB 1810
2370 GOSUB 4870
2380 GOSUB 2400
2390 GOTO 50
2400 OPEN"I",1,AY$
2410 FOR R=0 TO 31
2420 FOR C=0 TO 31
2430 INPUT #1,AY%(C,R,AY)
2440 NEXT C
2450 NEXT R
2460 CLOSE #1
2470 RETURN
2480 GOSUB 1790
2490 INPUT "KEY MAXIMUM ERROR (COMP UNITS)";E
2500 GOSUB 4870
2510 FOR R=0 TO 31
2520 FOR C=0 TO 31
2530 PP=AY%(C,R,AY):IF PP=0 THEN 2570
2540 EE=INT(RND*(2*E)-E)
2550 PE=PP+EE
2560 PP=64*(PE/64-INT(PE/64))+64
2570 AY%(C,R,AY)=PP
2580 Z$=INKEY$:IF Z$="A" THEN 290
2590 NEXT C
2600 NEXT R
2610 CLOSE #1:GOTO 50
2620 M=((15.5-R)^2+(C-15.5)^2)/2.4025
2630 IF M>84 THEN M=4:RETURN
2640 IF M>61 THEN M=3:RETURN
2650 IF M>36 THEN M=2:RETURN
2660 IF M>11 THEN M=1:RETURN
2670 M=0:RETURN
2680 JR=13
2681 FOR N=0 TO 4
2682 Y(N)=9
2683 NEXT N
2684 FOR N=0 TO 4
2685 LINE INPUT "ARRAY FILE # ";Y$
2686 IF LEN(Y$)=0 THEN 2693
2687 IF LEN(Y$)=1 THEN 2689
2688 PRINT "RE-DO FROM START":GOTO 2681
2689 R=ASC(Y$)
2690 IF R>52 OR R<48 THEN 2688
2691 Y(N)=VAL(Y$)
2692 NEXT N
2693 IF Y(0)=9 THEN 2688
2694 PRINT
2695 FOR N=0 TO 4
2696 PRINT USING "###";Y(N);
2697 NEXT N
2698 PRINT
2700 GOSUB 1840
2710 GOSUB 4870
2720 '
2730 FOR C=0 TO 31
2740 FOR R=0 TO 31
2750 Z$=INKEY$:IF Z$="A" THEN 290
2760 SS(C,R,0)=0:SS(C,R,1)=0
2770 NEXT R
2780 NEXT C
2790 FOR N=0 TO 4
2800 IF Y(N)>4 THEN 2920
2810 FOR C=0 TO 31
2820 FOR R=0 TO 31
2830 P=AY%(C,R,Y(N))
2840 IF P=0 THEN 2900
2850 P=.098175*(P-64)
2860 SS(C,R,0)=SS(C,R,0)+SIN(P)
2870 SS(C,R,1)=SS(C,R,1)+COS(P)
```

```
2880 PRINT N;C;R;P,SIN(P),COS(P),ATN(SS(C,R,0)/SS(C,R,1))
2890 Z$=INKEY$:IF Z$="A" THEN 290
2900 NEXT R
2910 NEXT C
2920 NEXT N
2930 PI=3.14159
2940 FOR C=0 TO 31
2950 FOR R=0 TO 31
2960 A=SS(C,R,0):B=SS(C,R,1)
2970 IF B=0 THEN 3040
2980 IF ABS(A/B)>1 THEN 3050
2990 IF B>0 THEN 3010
3000 X=PI+ATN(A/B):GOTO 3080
3010 IF A<0 THEN 3030
3020 X=ATN(A/B):GOTO 3080
3030 X=2*PI+ATN(A/B):GOTO 3080
3040 IF A=0 THEN X=-2*PI:GOTO 3080
3050 IF A<0 THEN 3070
3060 X=PI/2-ATN(B/A):GOTO 3080
3070 X=3*PI/2-ATN(B/A)
3080 X=64*X/(2*PI)
3090 IF JR<>19 THEN AY%(C,R,5)=INT(X)+64:GOTO 3130
3100 P=AY%(C,R,5)+INT(X)+128
3110 P=64*(P/64-INT(P/64))+64
3120 AY%(C,R,5)=P
3130 PRINT A,B,X,P
3140 Z$=INKEY$:IF Z$="A" THEN 290
3150 NEXT R
3160 NEXT C
3220 FOR C=0 TO 31
3230 FOR R=0 TO 31
3240 IF T$<>"G" THEN AA=0: GOTO 3260
3250 GOSUB 2620: AA=M:IF AA>15 THEN AA=15
3260 X=(SS(C,R,0))^2+(SS(C,R,1))^2
3270 IF X=0 THEN AC=15:GOTO 3290
3280 AC=INT(AA-LOG(X)*1.73717728#+.5)
3290 SS(C,R,0)=AC
3300 PRINT C,R,AC,X
3310 Z$=INKEY$:IF Z$="A" THEN 290
3320 NEXT R
3330 NEXT C
3350 GOTO 50
3360 '
3370 OPEN"I",1,AY$
3380 FOR C=0 TO 31
3390 FOR R=0 TO 31
3400 INPUT #1,SS(C,R,0)
3430 NEXT R
3440 NEXT C
3450 CLOSE #1
3460 GOTO 50
3470 GOSUB 1770
3480 FOR C=0 TO 31
3490 FOR R=0 TO 31
3500 AC=SS(C,R,0)+A
3510 PRINT C,R,AC,
3520 FOR X=15 TO AC STEP -1
3530 IF X>=0 THEN PRINT"*";:GOTO 3550
3540 PRINT"=";
3550 NEXT X
3560 PRINT
3570 IF PR=1 THEN GOSUB 3760
3580 Z$=INKEY$:IF Z$="A" THEN 290
3590 NEXT R
3600 NEXT C
3610 S$="/a'^bwi*+=-.@#%"
3620 PRINT:PRINT:PRINT:PRINT:PRINT CHR$(27);"F":IF PR=1 THEN LPRINT:LPRINT:LPRINT:LPRINT:LPRINT CHR$(27);"I10m"
3630 FOR R=0 TO 31
3640 Z=0
3650 FOR C=0 TO 31
3660 Z$=INKEY$:IF Z$="A" THEN 290
3670 AC=SS(C,R,0)+A
3680 IF AC<1 THEN AC=1
3690 IF AC>15 THEN AC=15
3700 D$=MID$(S$,AC,1):PRINT D$;D$;:IF PR=1 THEN LPRINT D$;D$;D$;
3710 NEXT C
```

```
3720 PRINT:IF PR=1 THEN LPRINT:Z=Z+1:IF Z=1 THEN 3650
3730 NEXT R
3740 PRINT CHR$(27);"G":IF PR=1 THEN LPRINT CHR$(27);"[11m"
3750 GOTO 290
3760 LPRINT C,R,AC,
3770 FOR X=15 TO AC STEP -1
3780 IF X>=0 THEN LPRINT "*";:GOTO 3800
3790 LPRINT"=";
3800 NEXT X
3810 LPRINT:RETURN
3820 GOSUB 1770
3830 GOSUB 4870
3840 FOR C=0 TO 31
3850 FOR R=0 TO 31
3860 AC=SS(C,R,0):IF AC<0 THEN AC=0
3870 IF AC>15 THEN AC=15
3880 OUT 0,255:OUT 0,1:OUT 0,C:OUT 0,R:OUT 0,AC+A
3890 Z$=INKEY$:IF Z$="A" THEN 290
3900 NEXT R
3910 NEXT C
3920 GOTO 50
3930 GOSUB 1790
3940 INPUT "PHASE SHIFT";ADJ
3945 GOSUB 4870
3950 FOR C=0 TO 31
3960 FOR R=0 TO 31
3970 P=AY%(C,R,AY)
3980 IF P=0 THEN 4030
3990 P=128+P+ADJ
4000 P=64*(P/64-INT(P/64))+64
4010 AY%(C,R,AY)=P
4040 NEXT R
4050 NEXT C
4060 GOTO 50
4070 JR=18:GOTO 800
4080 JR=19:GOTO 2681
4090 GOSUB 1790
4100 GOSUB 1840
4110 GOSUB 1770
4120 GOSUB 4680
4130 OPEN "I",1,"RND"
4140 N=1
4150 PRINT:PRINT N-1,821-N,,
4160 INPUT "# TO LOAD?";X
4165 PRINT
4170 IF X=0 THEN GOTO 4290
4180 IF N+X>821 THEN 4150
4190 FOR NN=N+1 TO N+X
4200 INPUT #1,D:D=D/100
4210 R=INT(D):C=INT(100*(D-R)+.2)
4220 GOSUB 4430
4230 GOSUB 4460
4240 PRINT C,R,AY%(C,R,AY)-64,AA:IF PR=1 THEN LPRINT C,R,AY%(C,R,AY)-64,AA
4250 N=N+1
4260 Z$=INKEY$:IF Z$="A" THEN 290
4270 NEXT NN
4280 GOTO 4150
4290 CLOSE #1:GOTO 50
4300 CL=0:CH=0:PP=0
4310 FOR Q=1 TO 5
4320 P=INP(1)/4
4330 PP=PP+P
4340 IF P>-1 AND P<15 THEN CL=CL+1:GOTO 4360
4350 IF P>50 AND P<64 THEN CH=CH+1
4360 NEXT Q
4370 IF CL*CH=0 THEN 4390
4380 PP=PP+(CL*64)
4390 P=INT(PP/5+.5)
4400 P=64*(P/64-INT(P/64))+64
4410 RETURN
4420 REM
4430 P=AY%(C,R,AY)-64:IF P<0 THEN P=64
4440 OUT 0,255:OUT 0,1:OUT 0,C:OUT 0,R:OUT 0,P+64
4450 RETURN
4460 IF T$<> "G" THEN AA=A:GOTO 4480
4470 GOSUB 2620:AA=M+A
```

```
4480 IF AA >15 THEN AA=15
4490 IF AA<0 THEN AA=0
4500 OUT 0,255:OUT 0,1:OUT 0,C:OUT 0,R:OUT 0,AA
4510 RETURN
4520 GOSUB 1790
4530 GOSUB 1840
4540 GOSUB 1770
4550 GOSUB 4680
4560 PRINT
4570 INPUT "COL #";Z$:C=VAL(Z$):IF Z$="M" THEN 50
4580 IF C>31 THEN GOTO 50
4590 IF C<0 THEN 4570
4600 FOR R=0 TO 31
4610 GOSUB 4430
4620 GOSUB 4460
4630 Z$=INKEY$:IF Z$="A" THEN 290
4640 NEXT R
4650 GOTO 4570
4660 GOSUB 4680
4670 GOTO 50
4680 GOSUB 1750
4690 OUT 0,255:OUT 0,5:OUT 0,4*(F/2-1):RETURN
4700 F=15:OUT 0,255:OUT 0,5:OUT 0,4
4710 GOSUB 4870
4720 FOR T=1 TO 2
4730 FOR C=0 TO 31
4740 FOR R=0 TO 31
4745 Z$=INKEY$:IF Z$="A" THEN 290
4750 OUT 0,255:OUT 0,1:OUT 0,C:OUT 0,R:OUT 0,P
4760 NEXT R
4770 NEXT C
4780 P=64
4790 NEXT T:GOTO 50
4800 PRINT "DESTINATION ";:GOSUB 1810
4820 GOTO 4900
4830 PRINT "SOURCE ";:GOSUB 1810
4840 AY=5:GOSUB 2400
4850 AY$="A"+AY$
4860 GOTO 3360
4870 PRINT CHR$(27);"Y6H";"PROCESSING";:RETURN
4900 AY=5
4910 GOSUB 2070
4920 AY$="A"+AY$
4930 OPEN "O",1,AY$
4940 FOR C=0 TO 31
4950 FOR R=0 TO 31
4960 WRITE #1,SSIC,R,0)
4970 NEXT R
4980 NEXT C
4990 CLOSE #1:GOTO 50
```

SECTION III

RECOMMENDATIONS FOR ADDITIONAL AREAS OF WORK

We recommend the following as additional areas of work to be performed by the contractor as part of future efforts:

1) Design and fabricate a scanner hardware and software control, data acquisition, and processing system to provide antenna patterns from measurement data output by the Beam/Pattern Monitor and Display System. A host computer, terminal, monitor, and printer would be supplied by the contractor as part of the system.
2) Using the system developed in 1) above, develop a software system to generate far field antenna patterns from near field measurements made with the Beam/Pattern Monitor and Display System.
3) Provide maintenance and systems engineering support to NASA on the Sonic Simulator and Beam/Pattern Monitor and Display Systems.
4) Assist NASA in defining and investigating additonal Space Station antenna study areas. The effort could include but not be limited to multibeam phased array beamforming phase control using open loop, retrodirective, and/or interferomteric means. Such studies could also involve the use of the Sonic Simulator and Beam/Pattern Monitor Systems.

REFERENCES

1. R. C. Johnson, H.A. Ecker, and J. S. Hollis, "Determination of Far-Field Antenna Patterns from Near-Field Measurements," Proc. IEEE, vol. 61, no. 12, pp. 1668-1692, Dec. 1973.

2. J. Borowick, A. E. Holley, W. L. Lange, R. W. Howard, and R. L. Cummings, "A Near-Field Antenna Measurement System," IEEE Trans. Instrumentation and Meas., vol. IM-32, no. 1, pp. 91-102, Mar. 1983.

3. E. B. Joy, W. M. Leach, Jr., G. P. Rodrigue, and D. T. Paris, "Applications of Probe-Compensated Near-Field Measurements," IEEE Trans. Antennas Propagat., vol. AP-26, no. 3, pp. 379-389, May 1978.

4. H. G. Booker and P. C. Clemmow, "The Concept of an Angular Spectrum of Plane Waves, and Its Relation to That of Polar Diagram and Aperture Distribution," Proc. IEE, vol. 97, part III, pp. 11-17, Jan. 1950.

5. P. C. Clemmow , The Plane Wave Spectrum Representation of Electromagnetic Fields. Oxford, England: Pergamon, 1966.

6. C. W. Horton and G. S. Innis, "The Computation of Far-Field Radiation Patterns from Measurements Made Near the Source," J. Acoust. Soc. Am., vol. 33, no. 7, pp. 877-880, Jul. 1961.

7. D. D. Baker, "Determination of Far-Field Characteristics of Large Underwater Sound Transducers from Near-Field Measurements," J. Acoust. Soc. Am., vol. 34, no. 11, pp. 1737-1744, Nov. 1962.

8. C. A. Balanis, Antenna Theory Analysis and Design. New York: Harper and Row, 1982.

9. J. Brown and E. V. Jull, "The Prediction of Aerial Radiation Patterns from Near-Field Measurements," Proc. IEE, vol. 108B, pp. 635-644, Nov. 1961.

10. "Aperture Theory" in Microwave Scanning Antennas, R. C. Hansen, Ed., New York: Academic Press, 1964, pp. 31-32.

11. R. E. Collin and F. J. Zucker, Antenna Theory, Part 1. New York: McGraw-Hill, 1969.

12. D. T. Paris, W. M. Leach, Jr., and E. B. Joy, "Basic Theory of Probe-Compensated Near-Field Measurements," IEEE Trans. Antennas Propagat., vol. AP-26, no. 3, pp. 373-379, May 1978.

13. F. Jensen, "Electromagnetic Near-Field Far-Field Correlations," Ph.D. dissertation, Tech. Univ. of Denmark, Lyngby, July 1970.

14. Sonic Simulator Experiments and Multiple Beam Phased Array Concepts/Applications. Final Report, NASA contract NAS9-16506, Novar Electronics Corporation; pp. 1-62, 151-157, 215-219, March 28, 1983.

15. Solar Power Satellite Microwave Power Transmission and Reception. Proceedings of a workshop at Johnson Space Center, Houston, Texas, January 15-18, 1980; NASA Conference Publication 2141; pp. 139-140.

16. Sonic Simulator Design, Operations Report. NASA Contract NAS9-16506, Novar Electronics Corporation; pp. 27-47, March 28, 1983.

APPENDIX

ENVIRONMENTAL EFFECTS ON SONIC SIMULATOR MEASUREMENTS

A.1 EFFECT OF TEMPERATURE ON SONIC SIMULATOR EXPERIMENTS

The velocity of sound varies with temperature. Error can be introduced into near field measurements unless either the ambient temperature is held constant or else the frequency of operation is varied correspondingly with temperature to keep the wavelength constant. (The parameter of interest is phase - constant phase.) Therefore the sonic simulator is designed to vary its frequency output as a function of ambient temperature to maintain constant wavelength.

The equation governing the relationship between the velocity of sound at any temperature is given by

$$v \cong v_o \sqrt{1 + t/273} \quad * \qquad \text{(A-1)}$$

where t is in ^{o}C, and v_o is the velocity at $0^{o}C$. The wavelength, λ, is related to the velocity, v, and frequency of sound, f, by the relationship

$$\lambda = \frac{v}{f} . \qquad \text{(A-2)}$$

From the above two expressions we obtain the fact that at a fixed frequency, the wavelength changes about 0.2% for every $1^{o}C$ change in temperature:

$$\frac{\Delta v/v}{\Delta t} \cong \frac{1}{2} \cdot \frac{1}{273} = 0.0018.$$

*Handbook of Chemistry and Physics, 23rd Edition, p. 1884.

For most far field measurements and for all of those beam characteristics measured as a part of previous contracts with the sonic simulator, that particular magnitude change in wavelength has negligible effects. For example, with an array of fixed dimensions, beamwidth is proportional to wavelength. Thus, say, for a 10^{o}C rise in temperature, there is only about a 2% increase in wavelength and hence the effect on measured beamwidth is negligible. Thus temperature effects on wavelength appear to have negligible consequences for far field measurements--those that normally are taken only of amplitude in the focal plane, a plane of constant phase. However, to determine far field patterns from near field measurements, phase must be preserved accurately. During the time it takes to make a complete scan of the near field, the phase error must be held to a fraction of a wavelength. This means that the change in wavelength due to temperature changes that occur within a complete scan of the sound field must be kept small. For example, consider measurements made in a plane parallel to the sonic array when the array is on the order of 30 to 60 cm. away from the plane. A measurement point which for instance is 60 cm. or so from transducers on the array is on the order of 7 wavelengths away from those transducers ($1\lambda \tilde{=} 8.6$ cm. at 4kHz at room temperature.) For a 10^{o}C change in temperature, we get a change of:

$$10 \times 0.2\% \times 7\lambda = 14\% \times \lambda \cong 50^{o} \text{ change in phase.}$$

Error can thus be introduced into near field measurements unless either the ambient temperature is held constant or else the frequency is varied correspondingly with temperature to keep the wavelength constant.

Refer again to Equations (A-1) and (A-2). If frequency, f, is varied according to the relationship

$$f = f_o \sqrt{1 + t/273}, \qquad \text{(A-3)}$$

then λ will be constant and equal to v_o/f_o. Selecting f_o such that f = 4kHz at 25°C, and realizing that (A-3) is closely approximated by the linear expansion

$$f = f_o\left(1 + \frac{t}{546}\right) \qquad \text{(A-4)}$$

we see that if frequency is linearly compensated for temperature changes according to the expression in (A-4), then wavelength is kept constant. The sonic simulator circuitry is designed to vary its output frequency in a linear fashion over a temperature range of approximately 25°C (from about 10°C to 38°C).

A.2 EFFECTS OF HUMIDITY AND BAROMETRIC PRESSURE

The change in wavelength due to changes in humidity and barometric pressure is miniscule compared to changes due to temperature. This is because the velocity of sound

in air is such a weak function of those two variables, especially compared to temperature.